Archives of Microbiology (2025) 207:130
https://doi.org/10.1007/s00203-025-04324-0

ORIGINAL PAPER

Efficacy of ultraviolet-light emitting diodes in bacterial inactivation and DNA damage via sensitivity evaluation using multiple wavelengths and bacterial strains

Kai Ishida[1,2] · Mina Matsubara[3] · Miharu Nagahashi[3] · Yushi Onoda[1,3,4] · Toshihiko Aizawa[4] · Shigeharu Yamauchi[4] · Yasuo Fujikawa[4] · Tomotake Tanaka[4] · Yasuko Kadomura-Ishikawa[1,3] · Takashi Uebanso[1,3] · Masatake Akutagawa[5] · Kazuaki Mawatari[1,3] · Akira Takahashi[1,3]

Received: 14 January 2025 / Revised: 28 March 2025 / Accepted: 1 April 2025

Abstract

Ultraviolet-light emitting diodes (UV-LEDs) have garnered attention for their efficient bacterial inactivation. However, in previous studies, it has been difficult to strictly compare the bacterial inactivation effect of UV irradiation among wavelengths differing by a few nanometers because detailed UV irradiation conditions for comparison, such as the LED characteristics at each wavelength and power supply characteristics, have not been established. Therefore, this study aimed to evaluate UV inactivation of 10 bacterial strains across 13 wavelengths (250–365 nm) using a standardized irradiation system previously reported to identify the most effective wavelengths for prevention of bacterial infection and contamination. Bacterial inactivation dose response curves were generated to determine the fluence required to archive 1–3 $\log_{10}$ inactivation. The results indicated that Gram-negative bacteria exhibited higher initial sensitivity compared with Gram-positive bacteria. Wavelength-dependent inactivation peaked at 263–270 nm, correlating strongly with cyclobutane pyrimidine dimer production ($r > 0.9$ for most strains). Deconvolution analysis confirmed that bacterial inhibition was maximal around 267.6 nm. Furthermore, UV-LEDs outperformed low-pressure mercury lamps in terms of bacterial inactivation under equivalent fluences, attributed to differences in spectral emission profiles. These findings will help optimize UV-LED sterilization methods for broader applications in microbial control.

Keywords Bacterial photosensitivity · Cyclobutene pyrimidine dimer · Low-pressure mercury lamp · Ultraviolet-light emitting diodes · Winer deconvolution

Introduction

Bacteria are ubiquitous in nature and can be found in every conceivable habitat, including soil, plants, the sea, air, humans, animals, artificial materials, and even extreme environments such as acidic hot springs (Soni et al. 2004; Wibowo et al. 2023; Rappaport et al. 2023). They are often classified based on their various shapes and structures, such as spherical, rod-shaped, slightly curved rods or comma–shaped, spiral–shaped, and tightly coiled forms, as well as by the thickness of their peptidoglycan layer (Kysela et al. 2016; Vollmer et al. 2008). Many bacteria exist in human living environments, and some can have harmful effects via contact, oral, droplets, and airborne infections (Antunes et al. 2020; Wei et al. 2016). Given the prevalence of pathogenic bacteria in human living environments,

Communicated by Pankaj Bhatt.

✉ Akira Takahashi
akiratak@tokushima-u.ac.jp

1 Department of Microbial Control, Institute of Biomedical Sciences, Tokushima University Graduate School, Tokushima, Japan

2 Department of Infectious Disease, Graduate School of Medical Science, Kyoto Prefectural University of Medicine, Kyoto, Japan

3 Department of Preventive Environment and Nutrition, Institute of Biomedical Sciences, Tokushima University Graduate School, Tokushima, Japan

4 Nichia Corporation, Tokushima, Japan

5 Department of Electrical and Electronic Engineering, Graduate School of Technology, Industrial and Social Sciences, University of Tokushima, Tokushima, Japan

Published online: 25 April 2025

effective sanitation using various disinfection techniques is essential to maintain health and well-being.

General sterilization methods, such as heat, chemical treatments, ultraviolet (UV) radiation, ozone, and high-pressure steam, are widely employed across various fields (Bharti et al. 2022). Among these techniques, there is a growing demand for sterilization technologies that minimize chemical or physical impacts on the target, especially in environments where food or people are present (Park et al. 2021). For example, in 2000, the U.S. Food and Drug Administration approved UV radiation as an effective method for controlling pathogens in food, water, and beverages (Li et al. 2005). UV disinfection is a non-chemical method that produces few by-products while maintaining the nutritional quality of food. As a result, it is suitable not only for sterilizing human food and drinking water but also for disinfecting indoor environments. The inhibitory effects of UV radiation on microorganisms have been extensively studied using mercury-based lamps, such as low-pressure mercury (LP–Hg) and medium-pressure mercury lamps (Beck and Linden 2015; Chen et al. 2009; Oliveira et al. 2021; Rodríguez et al. 2022), as well as tunable wavelength lasers (Beck et al.2015; Beck et al. 2014; Schuit et al. 2022) and light-emitting diode (LED). Currently, LP–Hg lamps are the most widely used UV sources for microbial inhibition. However, due to restrictions and legislative bans on mercury use, there is an increasing shift towards safer alternatives, such as excimer lamps (Ning et al. 2023) and UV-LEDs. Of these, UV–LEDs have gained significant attention for their applications in water treatment, food sterilization, and indoor disinfection. This increasing interest is fueled by their vast breadth of wavelengths, compact size, versatile design, long lifespan, tunable output (regulated by driving current), and environmental advantages, such as the lack of hazardous waste like mercury (Kebbi et al. 2020; Martín-Sómer et al. 2023; Song et al. 2016; Taghipour 2018; Wan et al. 2022). So far, many studies have reported on microorganism inactivation by UV–LED irradiation (Masjoudi et al. 2021). To accurately compare and evaluate UV sensitivity across different bacterial species, it is crucial to standardize irradiation–related conditions such as peak wavelength, irradiance, beam angle, bottom surface reflection, the presence or absence of a stirrer, sample temperature, and sample volume during exposure (Bolton et al. 2015; Beck and Linden 2015). Protocols for LED irradiation have been described in a few report (Kheyrandish et al. 2018; Sholtes et al. 2019). However, there are no published protocols establishing the experimental conditions for UV sensitivity evaluation using UV-LEDs based strictly on their optical characteristics, such as temperature-dependent peak wavelength shifts, temperature versus relative radiation flux characteristics, and power supply factors including overshoot and time delay. In our previous study, we developed an irradiation system that takes into consideration the LED and power supply characteristics; using this system, we then established a standardized evaluation method, and elucidated UV sensitivity across LEDs of 13 different wavelength (from U250 to U365) for fungi, as well as UV tolerance due to melanin (Ishida et al. 2024; Onoda et al. 2024). Following these studies, comparing UV sensitivity among bacterial strains could reveal the most effective UV wavelengths for preventing contamination of specific strains.

To compare the UV bacterial inactivation at various wavelengths, we need to evaluate bacteria present in human environments with different structures, survival environments, and pathogenicities. *Escherichia coli* is a widely used experimental model for bacteria and is found in soil and the intestinal tracts and feces of animals. In addition, the incidence of extended-spectrum beta-lactamase-producing *E. coli*, a type of drug-resistant bacteria, has increased in recent years (Erkan et al. 2025). *Staphylococcus aureus*, a foodborne pathogen, is commonly found on human skin, particularly the fingers, and it can cause food poisoning via contaminated food during the cooking process (Liu et al. 2022). Similarly, there are drug-resistant strains of *Pseudomonas aeruginosa* and *Enterococcus faecalis*, which pose a risk of nosocomial infection, along with *E. coli* and *S. aureus* (Cascante et al. 2025; Dadashi et al. 2021; Pham et al. 2019). *Salmonella enterica* Enteritidis, *Campylobacter jejuni*, and *Vibrio parahaemolyticus*, widely known as food-poisoning bacteria, are present in environments such as soil, oceans and animal intestines, and can cause digestive symptoms such as diarrhea and abdominal pain in infected humans (Delahoy et al. 2022; Vetchapitak et al. 2019). *Legionella pneumophila* is primarily found in soil and water environments and can cause pneumonia-like symptoms in humans contaminated via water ingestion or droplet inhalation (Iliadi et al. 2022). *Bacillus subtilis* and *Lactoplantibacillus plantarum* are opportunistic bacteria found in soil and food that have attracted attention for their use as probiotics (Chen et al. 2023). *B. subtilis* forms spore bodies and adapts to various stressors, making it more difficult to remove compared with other bacteria (Pedraza-Reyes et al. 2024). Based on the above, we selected *E. coli*, *S. enterica* Enteritidis, *C. jejuni, P. aeruginosa, L. pneumophila, S. aureus, E. faecalis*, *L. plantarum, B. subtilis* trophozoite, and *B. subtilis* spore to evaluate the inactivation effect of UV irradiation.

To acquire essential data for the development of device and methods to prevent bacterial infection and contamination, in this study, we aimed to compare the effects of our developed irradiation system on inactivation of various bacteria and to explore the most effective UV wavelengths for inactivation. From our results, we identified differences in UV sensitivity among these bacteria, determined the most

effective wavelengths for inhibition, established a correlation between bacterial inactivation specifically in the UVC region and the degree of DNA damage, and revealed differences in bacterial inactivation and DNA damage between LED and LP-Hg lamps under the same irradiation conditions. Under the same irradiation conditions, we compared inactivation of various bacterial strains exposed to UV-LEDs of wavelengths differing by only few nanometers. Our findings may contribute to the development of UV irradiation devices and methods with more effective bacterial inactivation.

Materials and methods

Bacterial strains and culture conditions

After preculturing from frozen stocks, *E. coli* ATCC 25922 (American Type Culture Collection (ATCC), Manassas, VA, USA), *S. aureus* ATCC 29213 and *S. enterica* serovar Enteritidis 171 strains (Nakano et al. 2012) were cultured in 1% NaCl–LB broth (1% tryptone, 0.5% yeast extract) at 37 ℃ for 24 h with shaking (170 rpm) until reaching the stationary phase. The culture medium was washed three times with D–phosphate buffered saline (D-PBS (−); Fujifilm Wako Chemicals, Osaka, Japan) followed by centrifugation at 12,000 rpm for 3 min per wash to remove the broth. The bacteria were evaluated by colony forming unit (CFU) assay using 1% NaCl–LB agar plates (Mori et al. 2007). *C. jejuni* NCTC11168 strain ATCC 700819 was cultured from frozen stocks in Muller-Hinton broth (#225,250; BD Difco, USA) at 37℃ under static and microaerobic conditions (5% O_2, 10% CO_2, 85% N_2) for 48 h. After centrifugation at 12,000 rpm for 3 min, the bacterial pellet was resuspended in fresh Muller-Hinton broth and incubated for an additional 36 h. The bacteria were then collected by centrifugation at 3,000 rpm for 15 min, and the pellet was washed with D-PBS. The bacteria were evaluated by CFU assay using MH agar plates (Fukushima et al. 2022). After preculturing from frozen stocks, *P. aeruginosa* PAO1 strain ATCC BAA–47 and *B. subtilis* IFO 3134 (Institute for Fermentation, Osaka, Japan) were cultured in Trypticase soy broth at 37 ℃ for 24 h with shaking (170 rpm) until reaching the stationary phase. The culture media were washed three times with D-PBS, by centrifugation at 12,000 rpm for 3 min per wash to remove the broth. *B. subtilis* was incubated in Trypticase soy broth at 37 °C for 24 h and then incubated at 37 °C for 7 days to allow sporulation. Subsequently, *B. subtilis* spore was harvested by washing with D-PBS three times, heating at 80 °C for 12 min to inactivate the vegetative and germinating cells, and washing again with D-PBS six times sequentially. The bacteria were evaluated by CFU assay using Trypticase soy agar plates (Hritonenko et al. 2018; Rattanakul et al. 2018). After preculturing from frozen stocks, *L. pneumophila* ATCC 33152 was cultured in BCYEα (buffered charcoal yeast extract with 0.1% α-ketoglutarate) broth at 37 ℃ for 48 h with shaking (170 rpm) until reaching the stationary phase. The culture medium was washed three times with D-PBS by centrifugation at 12,000 rpm for 3 min per wash to remove the broth. The bacteria were evaluated by CFU assay using BCYEα agar plates (Rattanakul et al. 2018). After preculturing from frozen stocks, *E. faecalis* ATCC 7080 was cultured in brain heart infusion broth (#237500; BD Difco) at 37 ℃ for 48 h under static conditions until reaching the stationary phase. The culture medium was washed three times with D-PBS by centrifugation at 12,000 rpm for 3 min per wash to remove the broth. The bacteria were evaluated by CFU assay using brain heart infusion agar plates (Kundra et al. 2021). After preculturing from frozen stocks, *L. plantarum* ATCC 8014 was cultured in De Man Rogosa Sharpe broth (#288,130; BD Difco) at 37℃ for 48 h under static condition until reaching the stationary phase. The culture medium was washed three times with D-PBS by centrifugation at 12,000 rpm for 3 min per wash to remove the broth. The bacteria were evaluated by CFU assay using De Man Rogosa Sharpe agar plates (Mežnarić et al. 2022). After preculturing from frozen stocks, *V. parahaemolyticus* RIMD 2210633 (Research Institute for Microbial Diseases (RIMD), Osaka University, Osaka, Japan) was cultured in 3% NaCl-LB broth at 37 ℃ for 24 h with shaking (170 rpm) until reaching the stationary phase. The culture medium was washed three times with D-PBS by centrifugation at 12,000 rpm for 3 min per wash to remove the broth. The bacteria were evaluated by CFU assay using 3% NaCl-LB agar plates (Ishida et al. 2023). Subsequently, to exclude weakening of the UV inactivation effect due to decreased permeability of the bacterial solution, all bacterial suspensions were diluted with D-PBS until reaching an absorbance at 600 nm (A_{600}) of 0.5, and the adjusted bacterial solutions were diluted tenfold for the UV irradiation experiments.

UV irradiation using the LEDs

UV irradiation was performed using a previously reported standardized UV-LED irradiation system, designed with consideration of the electrical and thermal characteristics of LEDs (Ishida et al. 2024). This system comprises a power supply, a timer to regulate LED activation, a chiller for temperature control, and a UV device consisting of a body and UV-LEDs portions of LEDs of 13 wavelengths (Nichia Corporation, Tokushima, Japan).

As described in our previous study, the device body was coated with a low-reflection material on all surfaces and equipped with three apertures between the LED and petri dish to minimize internal reflections of stray light. The number and arrangement of the LEDs were optimized via

optical simulations, ensuring stable irradiance with high uniformity. These simulations were performed to determine LED placement and irradiation distance, maintaining irradiance uniformity above 95% within a 20° range of oblique incident light. In addition, this device reduces irradiation time errors, and power supply characteristics such as time lag and overshoot. The UV-LED properties (temperature vs. peak wavelength, temperature vs. radiation flux, and current vs. peak wavelength) were measured, and the irradiance of each LED was determined based on these characteristics. At the same time, the irradiance of this device was confirmed by radiometer measurements calibrated by the Japan Calibration Service System (JCSS) and we confirmed that these values were in agreement within a 10% margin of error. In this device, the 13 wavelength-ranked LEDs (U250, U254, U257, U260, U263, U267, U270, U275, U280, U290, U300, U308, U365; Nichia Corporation, Tokushima, Japan) were evaluated for their inactivation effect on each bacterium. The peak wavelengths of each UV-LED in this study, as determined in our previous study, were as follows: 250.8 nm (U250 LED), 253.3 nm (U254 LED), 255.7 nm (U257 LED), 260.3 nm (U260 LED), 263.0 nm (U263 LED), 266.8 nm (U267 LED), 269.3 nm (U270 LED), 274.0 nm (U275 LED), 281.3 nm (U280 LED), 289.7 nm (U290 LED), 300.2 nm (U300 LED), 307.5 nm (U308 LED), and 367.0 nm (U365 LED). The spectral widths at half maximum of all LEDs used were in the range of ± 10 nm. The UV irradiance at the surface of the sample solution was unified to 1 mW/cm^2, except for 0.5 mW/cm^2 for U250, 1.5 mW/cm^2 for U290 and 18 mW/cm^2 for U365.

Each bacterial sample was prepared in D-PBS and then 1 mL of the prepared suspension was dispensed into a 35 mm dish (Sarstedt, Nümbrecht, Germany). The device conditions for UV irradiation were as follows: working distance, 100 mm; suspension volume, 1 mL; bacterial volume in the suspension, $A_{600} = 0.5$ with a tenfold dilution; no stirring. The dose-dependent inactivation effect was evaluated at fluences of 0, 2, 4, 6, 8, 10, 20, 30, 35, 40, 50, and 60 mJ/cm^2 using the U280 LED, and then the effect of irradiation at the other 12 wavelengths was compared at the integrated light fluence at which each bacterium was reduced by a factor of 1 $\log_{10}$ inactivation. All UV irradiation experiments were conducted in complete darkness to minimize the effects of ambient light, including potential photoreactivation by photolyases. The temperature of the bacterial samples was maintained at 25 °C by connecting a heat sink to a chiller positioned beneath the sample stage.

UV irradiation by using an LP-Hg lamp

UV lamp irradiation was conducted using an LP–Hg lamp with a flat-plate collimator (Blatchley et al. 1997; Shen et al. 2005). This collimator was designed to reduce reflection and transform the transmitted radiation into a nearly collimated beam. The LP–Hg lamp exhibited a peak wavelength of 253.4 nm with a spectral width at half maximum of ± 1.5 nm. The average irradiance at a distance of 125 mm from the base of the collimator tube was measured at 0.2 mW/cm^2, with fluctuations ranging from 0.08 to 0.35 mW/cm^2 over a 120-Hz cycle. Additionally, a minor fraction of radiation was emitted within the 300–600 nm wavelength range. Therefore, the irradiance contribution from the 300–600 nm range was quantified using an optical cut filter and subsequently subtracted, ensuring an irradiance of 0.2 mW/cm^2 at around 254 nm. The bacterial samples were suspended in D-PBS, and 1 mL of the suspension was transferred into a 35-mm dish. All UV irradiation experiments were conducted in complete darkness to minimize the effects of ambient light, including potential photoreactivation by photolyases. The temperature of the bacterial samples was maintained at 25 °C by connecting a heat sink to a chiller positioned beneath the sample stage.

Pulsed irradiation using the LEDs

Pulsed irradiation was controlled using a bipolar power supply (NF Corporation, Kanagawa, Japan) such that irradiance fluctuated from 0.08 to 0.35 mW/cm^2 over a 120–Hz cycle. All other conditions were the same as the continuous irradiation conditions. To simulate the intensity fluctuations, the emission intensities of the LEDs and LP-Hg lamp irradiation system were confirmed to be the same using a photodetector oscilloscope system.

Evaluation of inactivity effect for UV irradiated bacteria

The irradiated bacterial sample were recovered from 35 mm dish and diluted with D-PBS, and then 100 µL aliquots were plated on the appropriate agar plates. These plates were incubated under the specific conditions required for each bacterium. Bacterial counts were estimated by CFU assay. The value of inactivation was determined by the $\log_{10}$ reduction in CFUs compared with the non-irradiated bacterial sample. This value was defined as the "a factor of $\log_{10}$ inactivation" and was calculated using the following equation: a factor of $\log_{10}$ inactivation $= \log_{10}(Nt/N0)$, where Nt and No represent the CFU/mL of the UV–irradiated and non–irradiated samples, respectively.

Measurement of cyclobutene pyrimidine dimers and 6,4-photoproducts (6,4-PPs)

The CPD and 6,4–PP contents were measured using a high-sensitivity CPD ELISA kit (NM-MA-K003; Cosmo Bio Cat)

and 6,4-PP ELISA kit (NM-MA-K002; Cosmo Bio Cat), respectively. Genomic DNA was purified using DNeasy Blood and Tissue kits for DNA isolation (Qiagen, Hilden, Germany) after UV irradiation. For CPD measurement, the DNA samples were diluted to 0.4 µg/mL, and CPDs were detected using the CPD–specific monoclonal antibody clone TDM-2. For 6,4-PP measurement, the DNA samples were diluted to 4 µg/mL, and 6,4–PPs were detected using the 6,4–PP specific monoclonal antibody clone 64 M–2. Subsequently the samples were treated with a biotinylated secondary antibody, streptavidin peroxidase complex, and o-phenylenedidiamine to determine the amount of product complexed with the TDM–2 or 64 M–2 antibody. The reaction of peroxidase, H_2O_2 and o-phenylenediamine results in an orange color, and the color intensity is generally proportional to the amount of CPD or 6,4–PP in the sample. The chromogenic reaction was stopped, and the absorbance at 492 nm was measured using a microplate reader (SpectraMax i3; Molecular Device, Osaka, Japan).

Measurement of 8–hydroxy–2′–deoxyguanosine (8–OHdG)

The content of 8-OHdG was measured using a highly sensitive ELISA kit for 8–OHdG (KOG-HS10/E; Japan Institute for the Control of Aging, NIKKEN SEIL Co, Ltd, Tokyo, Japan). Genomic DNA was purified using the DNeasy Blood and Tissue kits for DNA isolation (Qiagen) after UV irradiation. Before measurement, the sample DNA was stimulated hydrolytically using the 8–OHdG Assay Preparation Reagent Set (#292–67801; Fujifilm Wako Chemicals). The isolated sample was diluted to 90 µg/mL, and 8–OHdG was detected using an 8–OHdG specific monoclonal antibody. The chromogenic reaction was stopped, and the absorbance at 450 nm was measured using a microplate reader (SpectraMax i3).

Expression analysis using SDS–PAGE and native–PAGE

The irradiated bacterial samples were centrifuged (12,000 rpm, 4 °C, 10 min) and the pellets resuspended in 300 µL radioimmunoprecipitation assay buffer (pH 7.4; 50 mM Tris HCl, 150 mM NaCl, 1 mM EDTA, 1% sodium deoxycholate, 0.1% SDS, 1% Triton X–100) and 30 µL 10 mg/mL achromopeptidase solution. After 1 h incubation at 4 °C with rotation, the bacterial suspension was homogenized sufficiently using a homogenizer. The mixture was centrifuged (12,000 rpm, 4 °C, 10 min) and the supernatant collected. The samples for SDS–PAGE were mixed with 5 × loading buffer (pH 6.8; 250 mM Tris–HCl, 50% glycerol, 5% SDS, bromophenol blue, 25% 2-mercaptoethanol) and boiled for 5 min at 95 °C. The samples for native–PAGE were mixed with 4 × loading buffer (200 mM Tris–HCl, 40% glycerol, bromophenol blue, pH 6.8) without boiling. The samples were then loaded onto each gel. Electrophoresis for SDS–PAGE was performed at room temperature for approximately 45 min using a constant current (20 mA) in 1 × running buffer (50 mM Tris base, 192 mM glycine, 0.1% SDS, pH 8.5) until the dye front reached the end of the gel. Electrophoresis for native–PAGE, electrophoresis was performed at 4 °C for approximately 60 min using a constant current (15 mA) in 1 × running buffer (Positive; 100 mM Tris–HCl, pH 7.8 / Negative; 53 mM Tris–HCl, 68 mM glycine, pH 8.9) until the dye front reached the end of the gel.

SDS-PAGE and native-PAGE gels were stained using 50 mL Coomassie Brilliant Blue solution (50% methanol, 10% acetic acid containing 0.025% Coomassie R–250) for 30 min and then destained in 100 mL of ddH_2O overnight using sharker.

Bacterial growth curve after UV irradiation

The optical densities of *E. coli*, *S. aureus, V. parahaemolyticus, C. jejuni, E. faecalis and B. subtilis* were measured using a microplate reader (SpectraMax i3) at a wavelength of 600 nm after UV–LED irradiation using U254, U260, U267, U270, U280, U308 and U365 LEDs. The irradiated bacterial samples (200 µL) were inoculated into a 12-well microplate containing 1800 µL each bacterial culture medium. The cultures without *C. jejuni* were incubated at 37 °C with shaking at 140 rpm, while A_{600} readings were recorded at 2 h intervals for 24 h. The culture of *C. jejuni* was incubated at 37 °C with static and microaerobic conditions (5% O_2, 10% CO_2, 85% N_2), while A_{600} readings were recorded at 6 h intervals for 48 h. The resulting values were used to construct bacterial growth curves.

Wiener deconvolution

UV-LED-induced inactivation of *E. coli* was evaluated using experimental data obtained from 13-wavelength UV-LEDs. The factor of $\log_{10}$ inactivation of *E. coli* under monochromatic light exposure at wavelength λ and radiant energy W, denoted as $k_L^{single}(\lambda)$, was estimated using the Wiener deconvolution method (Winer 1949; Press et al. 1992). The calculation formulae and methods employed for the estimation are outlined below:

The terms used in the calculation formulae are defined in Table S5. Based on these terms, $k_L^{single}(\lambda)$ is expressed as follows:

$$k_L^{single}(\lambda) = -\eta_L^{single}(\lambda)W \quad (1)$$

Here, $\eta_{\mathrm{L}}^{\mathrm{single}}(\lambda)$ represents the rate of reduction in the factor of $\log_{10}$ inactivation under monochromatic light at wavelength λ. In the case of LEDs, the spectral output was not a discrete line spectrum but rather a narrowband emission spectrum with a finite bandwidth. Taking this characteristic into account, the factor of $\log_{10}$ inactivation under a narrowband light source, such as an LED, denoted as $k_{\mathrm{L}}^{\mathrm{narrow}}$, can be expressed as follows:

$$k_L^{narrow}(\lambda) = \int_0^\infty k_L^{\sin gle}(\lambda) w(\lambda) d\lambda \tag{2}$$

$$= -\int_0^\infty \eta_L^{\sin gle}(\lambda) w(\lambda) d\lambda \tag{3}$$

The central wavelength of each LED was denoted as λ_c . The factor of $\log_{10}$ inactivation for an LED with central wavelength λ_c, denoted as $k_{\mathrm{L}}^{\mathrm{narrow}}(\lambda c)$, incorporating the spectral radiant energy of the light source at λ_c and the measurement error, could be expressed as follows:

$$k_{\mathrm{L}}^{\mathrm{narrow}}\left(\lambda_c\right) = W \int_0^\infty k_{\mathrm{L}}^{\mathrm{single}}(\lambda) h_0(\lambda_c - \lambda) d\lambda + n(\lambda_c) \tag{4}$$

By applying the Fourier transform to this equation with respect to λ_c, it could be expressed as follows:

$$K_{\mathrm{L}}^{\mathrm{narrow}}\left(\Lambda_c\right) = W K_{\mathrm{L}}^{\mathrm{single}}\left(\Lambda_c\right) H_0\left(\Lambda_c\right) + N\left(\Lambda_c\right) \tag{5}$$

Let $G\left(\Lambda_c\right)$ represent the Wiener deconvolution filter used to estimate $K_{\mathrm{L}}^{\mathrm{single}}\left(\Lambda_c\right)$. The filter $G\left(\Lambda_c\right)$ was expressed as follows (Vaseghi 2008; Thomas et al. 2016):

$$G\left(\Lambda_c\right) = \frac{H_0\left(\Lambda_c\right)}{\left|H_0\left(\Lambda_c\right)\right|^2 + \alpha} \tag{6}$$

At this point, the constant (α) was defined as follows:

$$\alpha = \frac{N\left(\Lambda_c\right)}{S\left(\Lambda_c\right)} \tag{7}$$

Using the Wiener deconvolution filter, the estimated value of the factor of $\log_{10}$ inactivation under monochromatic light exposure at wavelength λ and radiant energy W, after Fourier transformation ($\widehat{K_{\mathrm{L}}^{\mathrm{single}}}\left(\Lambda_c\right)$), was expressed as follows:

$$\widehat{K_{\mathrm{L}}^{\mathrm{single}}}\left(\Lambda_c\right) = G\left(\Lambda_c\right) K_{\mathrm{L}}^{\mathrm{narrow}}\left(\Lambda_c\right) \tag{8}$$

The estimated factor of $\log_{10}$ inactivation under exposure to monochromatic light of wavelength λ and radiation energy W, denoted as $\widehat{k_{\mathrm{L}}^{\mathrm{single}}}(\lambda)$, was calculated by applying the inverse Fourier transform to the estimated value $\widehat{K_{\mathrm{L}}^{\mathrm{single}}}\left(\Lambda_c\right)$.

Statistical analysis

All experiments were conducted in triplicate and on three separate days. The data were presented as the means ± standard error of the means for all experiments. Significant differences between two groups were calculated using Student's t test, with the threshold for significance set at a P value of 0.05 or 0.01. Significant differences among multiple groups were determined using one-way analysis of variance (ANOVA) and Tukey's honestly significant difference test in IBM SPSS Statistics 25 (SPSS Inc., Chicago, IL, USA): $P < 0.05$ was considered significant. The correlation between bacterial inactivation effects by UV irradiation and CPD production was assessed via a two-tailed significance test using Pearson's and Spearman's coefficients.

The UV dose response data in this study were fitted to the Weibull model (Mafart et al. 2002; Murat et al. 2023). GinaFit, an Excel plug-in developed by Gereeard et al. (2005) was used to solve for delta and P value.

$$\frac{N}{N_0} = 10^{\left(-\left(\left(\frac{t}{\delta}\right)^p\right)\right)} \tag{9}$$

The goodness of fit of the Weibull model was evaluated based on the root mean squared error between the measured and predicted factor of $\log_{10}$ inactivation values.

$$RMSE = \sqrt{\frac{\sum_{i=1}^{n}\left(LI_{pred} - LI_{obs}\right)^2}{n}} \tag{10}$$

Results

Each bacterial strain exhibited fluence-dependent individual inactivation when irradiated with the U280 LED

To investigate the UV sensitivity of bacteria under the uniformed irradiation condition, we first measured the dose-dependent inactivation effect of LED irradiation on individual bacterium. The ten bacteria evaluated in this study exhibited dose-dependent inactivation under U280 LED irradiation, but the inactivation effects at the same UV fluence varied depending on the bacterial strain (Fig. 1, Table S1). In addition to linear response curves, sigmoid-like curves with shoulders were observed in some strains. Usually, a sigmoid curve has an S–shape with both a shoulder and tailing section; however, due to the detection limits of the UV fluence observed using this device, only the shoulder and linear curve were observed without a tailing section. To compare the inactivation effects at

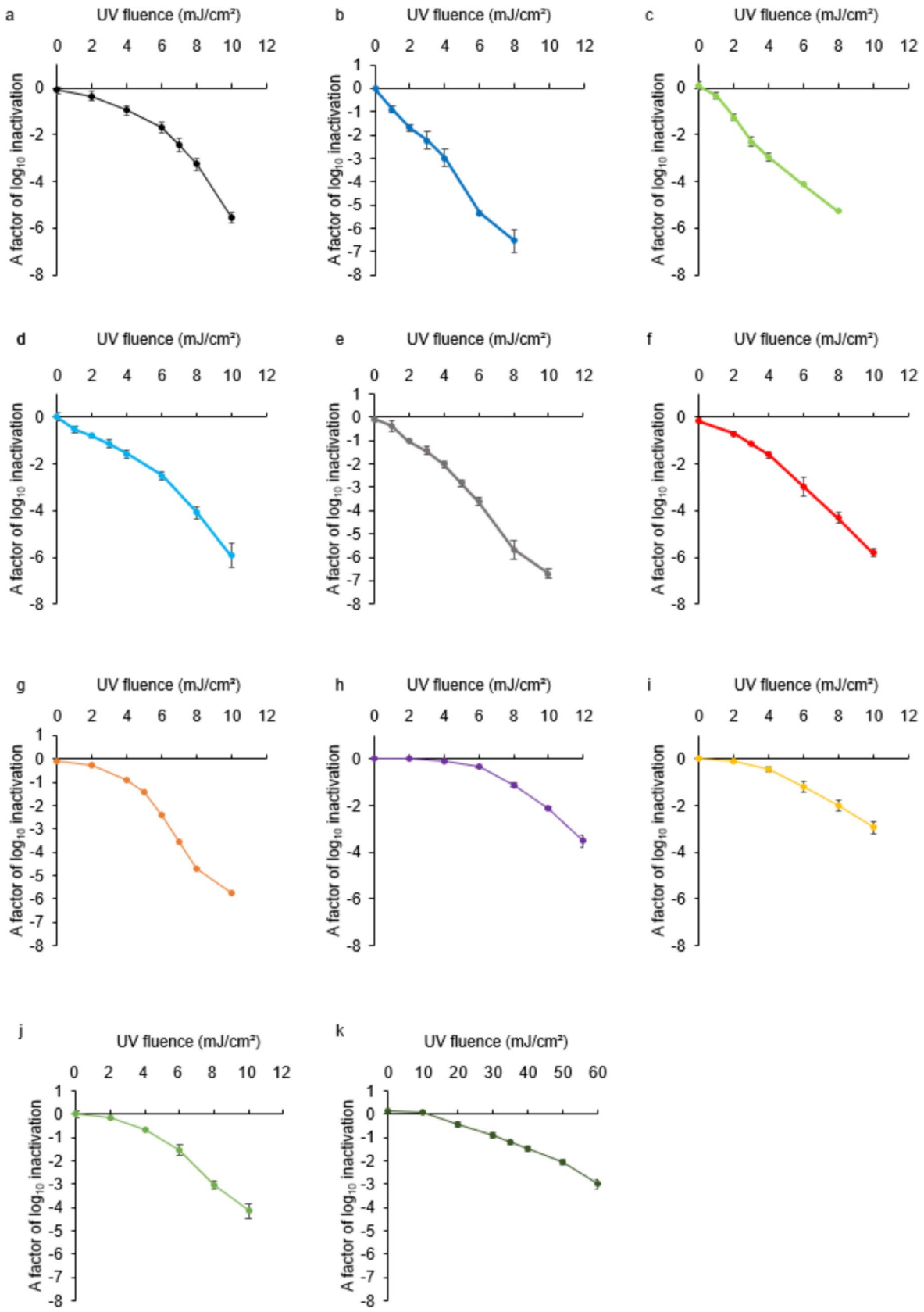

Fig. 1 Fluence response curves of the inactivation effect of each bacterium using the U280 LED

281.3 nm irradiation among the different bacterial strains, the UV fluence required for 1–3 log reductions and the inactivation rate constants calculated from the linear part of the dose–response curves of each microorganism were determined (Table 2). The UV fluence required for 1–3 log reductions were determined from the predicted curves generated using the Weibull model, based on the observed inactivation values and irradiation times. The root means square errors of the predicted values relative to the observed values are shown in Table S2. The inactivation rate constants calculated from the observed values were defined as two slopes: K_1, the initial inactivation rate constant corresponding to the shoulder section, and K_2, the log phase inactivation rate constant corresponding to the linear response curve. The results showed that Gram-negative bacteria except for *E. coli* required less UV fluence for 1–3 log reductions compared with Gram-positive bacteria. Additionally, while K_2 did not show a clear difference between Gram-negative and Gram-positive bacteria, except for *B. subtilis* spore, K_1 was higher for all Gram-negative than Gram-positive bacteria. These results suggest that structural differences such as peptidoglycan and the cell and outer membranes may influence the initial UV sensitivity at U280 LED irradiation (Table 1).

Bacterial suspensions were exposed to UV irradiation using the U280 LED at an irradiance of 1 mW/cm^2. The factor of $\log_{10}$ inactivation of each bacterium after UV irradiation was evaluated by the CFU assay. **a** *E. coli* was irradiated at fluences of 0, 2, 4, 6, 7, 8 and 10 mJ/cm^2, **b** *V. parahaemolyticus* was irradiated at fluences of 0, 1, 2, 3, 4, 6 and 8 mJ/cm^2, **c** *S. enterica* Enteritidis was irradiated at fluences of 0, 1, 2, 3, 4, 6 and 8 mJ/cm^2, **d** *C. jejuni* was irradiated at fluences of 0, 1, 2, 3, 4, 6, 8 and 10 mJ/cm^2, **e** *P. aeruginosa* was irradiated at fluences of 0, 1, 2, 3, 4, 5, 6, 8 and 10 mJ/cm^2, **f** *L. pneumophila* was irradiated at fluences of 0, 2, 3, 4, 6, 8 and 10 mJ/cm^2, **g** *S. aureus* was irradiated at fluences of 0, 2, 4, 5, 6, 7, 8 and 10 mJ/cm^2, **h** *E. faecalis* was irradiated at fluences of 0, 2, 4, 6, 8, 10 and 12 mJ/cm^2, **i** *L. plantarum* was irradiated at fluences of 0, 2, 4, 6, 8 and 10 mJ/cm^2, **j** *B. subtilis* trophozoite was irradiated at fluences of 0, 2, 4, 6, 8 and 10 mJ/cm^2, **k** *B. subtilis* spore was irradiated at fluences of 0, 10, 20, 30, 35, 40, 50 and 60 mJ/cm^2. Each bar indicates the mean concentration (n = 4/group).

Bacterial inhibition peaked at wavelengths around 263–270 nm when exposed to LEDs of 13 wavelengths

Next, UV sensitivity was compared among LEDs of 13 different wavelengths (U250, U253, U257, U260, U263, U267, U270, U275, U280, U290, U300, U308, and U365) to evaluate the wavelength dependency of bacterial UV sensitivity. The reference UV fluence for comparison was based on the UV fluence required for 1 log reduction under U280 LED irradiation for each bacterium, calculated in Fig. 1. The results showed a strong wavelength-dependent inhibitory effect within the 250–300 nm range, with all bacteria exhibiting an inactivation peak around 263–270 nm (Fig. 2). The maximum log reduction values were as follows: 2.79 ± 0.24 log for *E. coli*, 1.62 ± 0.09 log for *V. parahaemolyticus*, 2.04 ± 0.18 log for *S. enterica*, 1.75 ± 0.19 log for *C. jejuni*, 2.00 ± 0.36 log for *P. aeruginosa*, 2.17 ± 0.16 log for *L. pneumophila*, 2.20 ± 0.06 log for *S. aureus*, 4.28 ± 0.31 log for *E. faecalis*, 2.09 ± 0.17 log for *L. plantarum*, 2.74 ± 0.26 log for *B. subtilis* trophozoite, and 3.54 ± 0.13 log for *B. subtilis* spore (Table S3). *E. faecalis* exhibited significant differences within the UVC range, whereas *V. parahaemolyticus* and *C. jejuni* showed minor differences within the UVC range.

The rate of reduction by a factor of $\log_{10}$ inactivation under monochromatic light with the line spectrum $\eta_L^{single}(\lambda)$, represents the wavelength-dependent antimicrobial efficacy of a given target organism. This parameter provides

Table 1 UV fluence for a factor of 1–3 $\log_{10}$ inactivation and inactivation rate constants

Gram stain	Bacterial strain	$\log_{10}$ values			Inactivation rate constants	
		1 $\log_{10}$	2 $\log_{10}$	3 $\log_{10}$	K_1	K_2
Negative	*E. coli*	4.5	6.4	7.7	− 0.122 ± 0.018	− 0.766 ± 0.055
	V. parahaemolyticus	1.2	2.5	3.8	− 0.892 ± 0.204	− 0.858 ± 0.095
	S. enterica	3.0	4.8	6.5	− 0.515 ± 0.052	− 0.634 ± 0.051
	C. jejuni	2.1	3.7	5.2	− 0.297 ± 0.277	− 0.759 ± 0.033
	P. aeruginosa	1.8	3.0	4.4	− 0.451 ± 0.196	− 0.644 ± 0.033
	L. pneumophila	3.0	4.5	6.2	− 0.272 ± 0.069	− 0.673 ± 0.015
Positive	*S. aureus*	4.2	5.4	6.6	− 0.095 ± 0.045	− 0.864 ± 0.078
	E. faecalis	7.5	10.0	11.4	− 0.032 ± 0.013	− 0.528 ± 0.039
	L. plantarum	5.7	8.1	10.1	− 0.068 ± 0.032	− 0.413 ± 0.042
	B. subtilis trophozoite	4.5	6.7	8.3	− 0.093 ± 0.075	− 0.601 ± 0.063
	B. subtilis spore	36.0	48.0	61.0	− 0.003 ± 0.002	− 0.063 ± 0.005

valuable insight into the underlying bactericidal mechanisms. If $\eta_L^{single}(\lambda)$ is known, the antimicrobial efficacy of light sources with arbitrary wavelength spectra can be estimated. In principle, $\eta_L^{single}(\lambda)$ can be determined via sterilization experiments using monochromatic light sources, such as lasers, while scanning across different wavelengths. However, obtaining light sources that deliver high radiant energy across arbitrary wavelengths remains challenging. In practice, LEDs are a more feasible option, as they can readily produce high-output light at various wavelengths. Although LED emission spectra are typically narrowband, with full widths at half maximum ranging from a few nanometers to several tens of nanometers, they are not strictly monochromatic. To address this limitation, a signal processing approach was applied to estimate the wavelength-dependent reduction rate, $\eta_L^{single}(\lambda)$, based on the inactivation effects of multiple narrowband spectral light sources on *E. coli*. This analysis assumed that the factor of $\log_{10}$ inactivation was determined using light sources with identical spectral profiles but varying central wavelengths.

Deconvolution analysis was performed based on the inactivation effect of UV-LED irradiation on *E. coli* and the spectra obtained after padding (Fig. S6d). Due to the padding, the spectrum resulting from the deconvolution spanned approximately twice the wavelength range used in the experiment. However, values outside the measured range were extrapolated and thus considered less reliable. By trimming the deconvolution results to the experimentally measured range (Fig. S6e), four wavelengths corresponding to local minima were identified (Table S6). Among these, the most significant reduction in survival rate was observed at 267.6 nm. This finding aligns with the experimental results showing that UV-LED irradiation at a peak wavelength of 266.8 nm exhibited a strong inactivation effect on *E. coli* (Fig. 2a). These results provide detailed insight into the contribution of various UV wavelength bands to bacterial UV sensitivity. Additionally, they underscore the utility of deconvolution analysis for examining the wavelength-dependent reduction by a factor of $\log_{10}$ inactivation, as derived from inactivation data obtained using this irradiation system.

Bacterial inactivation by each UV-LED wavelength was correlated highly with DNA damage

Previous studies reported that UV light induces cell death by generating CPDs and 6–4PPs within the irradiated cellular DNA; these products disrupt the DNA structure, inhibit polymerases, and induce DNA replication (Rastogi et al. 2010; Lawrence et al. 2022). Such DNA damage is induced not only in human cells but also in pathogenic microorganisms (Kraft et al. 2011; Nyangaresi et al. 2023; Nascimento et al. 2010; Kuluncsics et al. 1999). Although DNA damage is observed across all UVA, UVB, and UVC wavelengths, the levels of DNA damage are significantly higher under UVB and UVC irradiation compared with UVA (Kuluncsics et al. 1999; Jiang et al. 2009). Therefore, we evaluated the production of CPD and 6,4-PP in irradiated bacteria under the conditions in Fig. 2 that demonstrated a wavelength–dependent inactivation effect around 250–300 nm (Fig. 3).

First, CPD production in the DNA of *E. coli* after exposure to the LEDs at 13 wavelengths was evaluated and compared with that under U280 LED irradiation. The results revealed varying levels of CPD production depending on the wavelength, with notably higher CPD production observed under UVC compared with UVA and UVB, and particularly high levels around 260 nm (Fig. 4a). Based on these findings, CPD production was further evaluated at 13 characteristic wavelength-ranked LEDs (U254, U260, U267, U270, and U280 LED) in other bacterial strain. First, it was evaluated in the Gram-negative bacteria *V. parahaemolyticus* and *C. jejuni*, which showed relatively weak inactivation. These bacteria exhibited comparable CPD production levels between U280 LED irradiation and the other wavelengths (Fig. 3b, c). Next, CPD production was evaluated in the Gram-positive bacteria *S. aureus*, *E. faecalis*, and *B. subtilis* trophozoite and spore. *S. aureus* and *B. subtilis* trophozoite exhibited particularly high CPD production around 267–270 nm (Fig. 3d, f). Although no significant differences were observed among the UVC wavelengths, *E. faecalis*, which showed relatively high inactivation, showed increased CPD production around 260–270 nm (Fig. 3e). In contrast, UV irradiation of *B. subtilis* spore resulted in CPD production similar to the level observed in the non-irradiated controls (Fig. 3g). Additionally, the production of 6,4–PPs, which is another type of DNA damage, was compared across different UV wavelengths using DNA from *E. coli* and *S. aureus*. 6,4–PP production varied depending on the wavelength, with particularly higher production observed under U267 and U270 than U280 LED irradiation (Fig. S1). The correlations between bacterial inactivation and CPD production at each UV wavelength are shown in Table 3. A strong positive correlation between bacterial inactivation and CPD production was observed in the bacteria evaluated. Furthermore, when regression lines were calculated and the coefficients of determination were assessed, all strains showed high accuracy with values > 0.5 (Table 2).

A previous study has reported that 8-hydroxy-2'-deoxyguanosine (8-OHdG) is an important biomarker of oxidative stress and is induced in UV irradiation, especially in the UVA region (Al-Sadek et al. 2024). Therefore, the involvement of 8–OHdG in bacterial inactivation was evaluated using DNA from *E. coli* and *S. aureus*. Under conditions inducing CPD and 6,4–PP production, there was no detectable increase in 8–OHdG production under irradiation compared with the

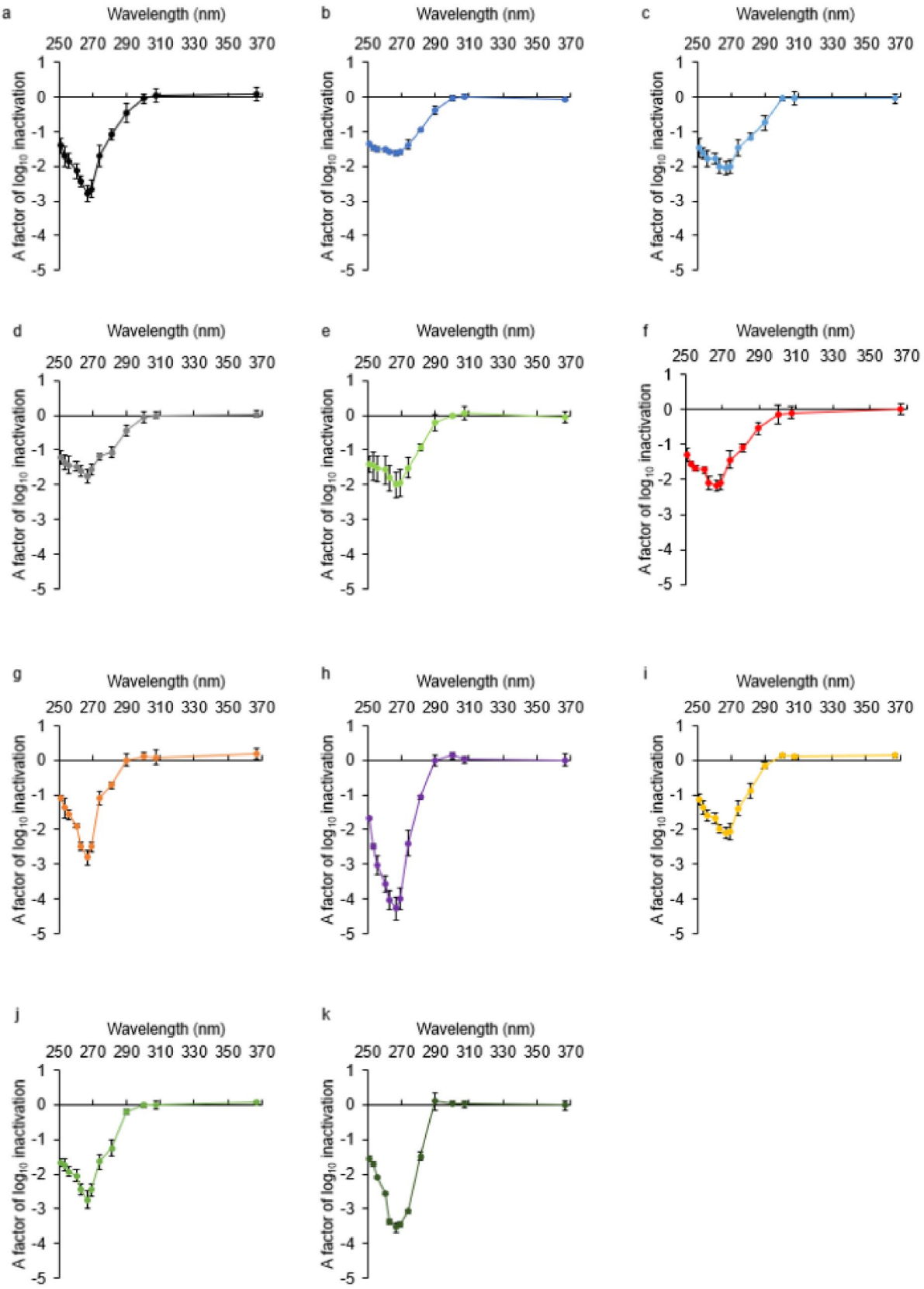
a
b
c
d
e
f
g
h
i
j
k
Wavelength (nm)
250 270 290 310 330 350 370
A factor of log10 inactivation
1 0 -1 -2 -3 -4 -5

◂**Fig. 2** The inactivation effect of 13 wavelength-ranked LEDs (U250, U254, U257, U260, U263, U267, U270, U275, U280, U290, U300, U308, and U365) on each bacterium. Bacterial suspensions were exposed to UV irradiation using 13 wavelength-ranked LEDs (U250, U254, U257, U260, U263, U267, U270, U275, U280, U290, U300, U308, and U365 LED) under fluence conditions that resulted in a 1 log reduction of each bacterium at U280 LED irradiation. The factor of $\log_{10}$ inactivation of each bacterium after UV irradiation was evaluated by CFU assay. **a** *E. coli* was irradiated at a fluence of 4.5 mJ/cm^2, **b** *V. parahaemolyticus* was irradiated at a fluence of 1.2 mJ/cm^2, **c** *S. enterica* Enteritidis was irradiated at a fluence of 3.0 mJ/cm^2, **d** *C. jejuni* was irradiated at a fluence of 2.1 mJ/cm^2, **e** *P. aeruginosa* was irradiated at a fluence of 1.8 mJ/cm^2, **f** *L. pneumophila* was irradiated at a fluence of 3.0 mJ/cm^2, **g** *S. aureus* was irradiated at a fluence of 4.2 mJ/cm^2, **h** *E. faecalis* was irradiated at a fluence of 7.5 mJ/cm^2, (i) *L. plantarum* was irradiated at a fluence of 5.7 mJ/cm^2, (j) *B. subtilis* trophozoite was irradiated at a fluence of 4.5 mJ/cm^2, and **k** *B. subtilis* spore was irradiated at a fluence of 36 mJ/cm^2. Each bar indicates the mean concentration (n = 4/group)

non–irradiated group (Fig. S2). Additionally, the effect of UV irradiation at each wavelength on the total intracellular protein levels was assessed using SDS-PAGE and native-PAGE. Similar to 8–OHdG, the changes were not observed on the amount of produced protein immediately after UV irradiation at used wavelength (Fig. S3). These results suggest that the inactivation of bacteria by UV irradiation is primarily driven by direct DNA damage, specifically CPD and 6,4-PP production. Moreover, the differences in bacterial inactivation among the wavelengths within the UVC range may be influenced by the production of these products.

UV-LEDs which emits peak wavelength of around 254 nm exhibited strong bacterial inactivation and DNA damage, compared with LP–Hg lamps

LP–Hg lamps, which emit monochromatic UV radiation at around 254 nm, have long been used as germicidal lamps and are widely used in the field of bacterial inhibition (Kebbi et al. 2020; Martín-Sómer et al. 2023). To compare the bacterial inhibitory effect between LP–Hg lamps and UV-LEDs, we used a device combining a LP–Hg lamp with a collimator tube. Additionally, we used the U254 LED adjusted to the same UV irradiance to adapt the same conditions because the UV irradiance of the LP–Hg lamp at the surface of the sample solution was 0.2 mW/cm^2. We compared inhibition between the LP-Hg lamp and U254 LED for *E. coli* and *S. aureus.* Both bacteria showed greater inactivation under U254 LED irradiation compared with the LP-Hg lamp. For *E. coli*, the inactivation at a UV fluence of 4 mJ/cm^2 was 0.88 ± 0.08 log under LP–Hg lamp irradiation versus 1.31 ± 0.27 log under U254 LED irradiation (Fig. 4a). For *S. aureus*, the inactivation at a UV fluence of 4 mJ/cm^2 was 0.08 ± 0.12 log under LP–Hg lamp irradiation versus 1.07 ± 0.14 log under U254 LED irradiation (Fig. 4b). In general, UV-LEDs emit continuous light, whereas LP-Hg lamps emit light of alternating intensities at regular intervals. With the LP-Hg lamp used in our device, irradiance varied from 0.08 to 0.35 mW/cm^2 over a 120–Hz cycle. To determine whether the difference in inactivation effects between the UV–LED and LP–Hg lamp was due to differences in the emission method, the UV–LED was modulated to emit light at the same frequency and amplitude as the LP–Hg lamp using a bipolar power supply, and *E. coli* and *S. aureus* inactivation were compared between the devices (Fig. 4, S4). UV–LED irradiation demonstrated greater bacterial inactivation under both the continuous and alternating emission modes compared with the LP–Hg lamp; no significant difference in inactivation was observed between the two emission modes of the UV–LED. To determine whether the difference in inactivation is related to CPD production, we evaluated inactivation and CPD production in bacteria irradiated at the same UV fluence as in Fig. 3. In *E. coli* and *S. aureus*, a difference in CPD production, which corresponded to the difference in inactivation, was observed between the UV–LED and LP-Hg lamp at the same peak wavelength (Fig. 4c–e). On the other hand, the similar CPD production was observed when the bacteria were irradiated at each UV fluence that produced the similar inactivation using the UV–LED or LP–Hg lamp (Fig. S5a–d). Additionally, similar evaluations were conducted for *V. parahaemolyticus* and *C. jejuni*, which exhibited relatively weak inactivation in comparison U267 LED with U280 LED in Fig. 2. *C. jejuni* showed decreased CPD production under conditions of differences in inactivation, and *V. parahaemolyticus* was observed to change in value of CPD production with no significant difference (Fig. 4g–j). We also irradiated at a UV fluence of 1 mW/cm^2 to assess the effect of UV fluence, but there was no difference in bacterial inactivation or CPD production in these bacteria (Fig. S5e–n). These findings indicate that the differences in bacterial inactivation between the UV–LED and LP-Hg lamp at the same UV fluence are dependent on CPD production.

The different UV-LED wavelengths affected bacterial growth after UV irradiation

Last, we evaluated bacterial growth after UV irradiance to reveal differences after irradiation at each wavelength. The measurements were conducted using seven wavelengths: five in the UVC range (U254, U260, U267, U270, and U280), one in the UVB range (U308), and one in the UVA range (U365). The growth ability of the bacteria after UV irradiation was evaluated under the UV fluence conditions required to achieve a factor of 1 $\log_{10}$ inactivation at each wavelength (Fig. 5). *E. coli, C. jejuni* and *E.*

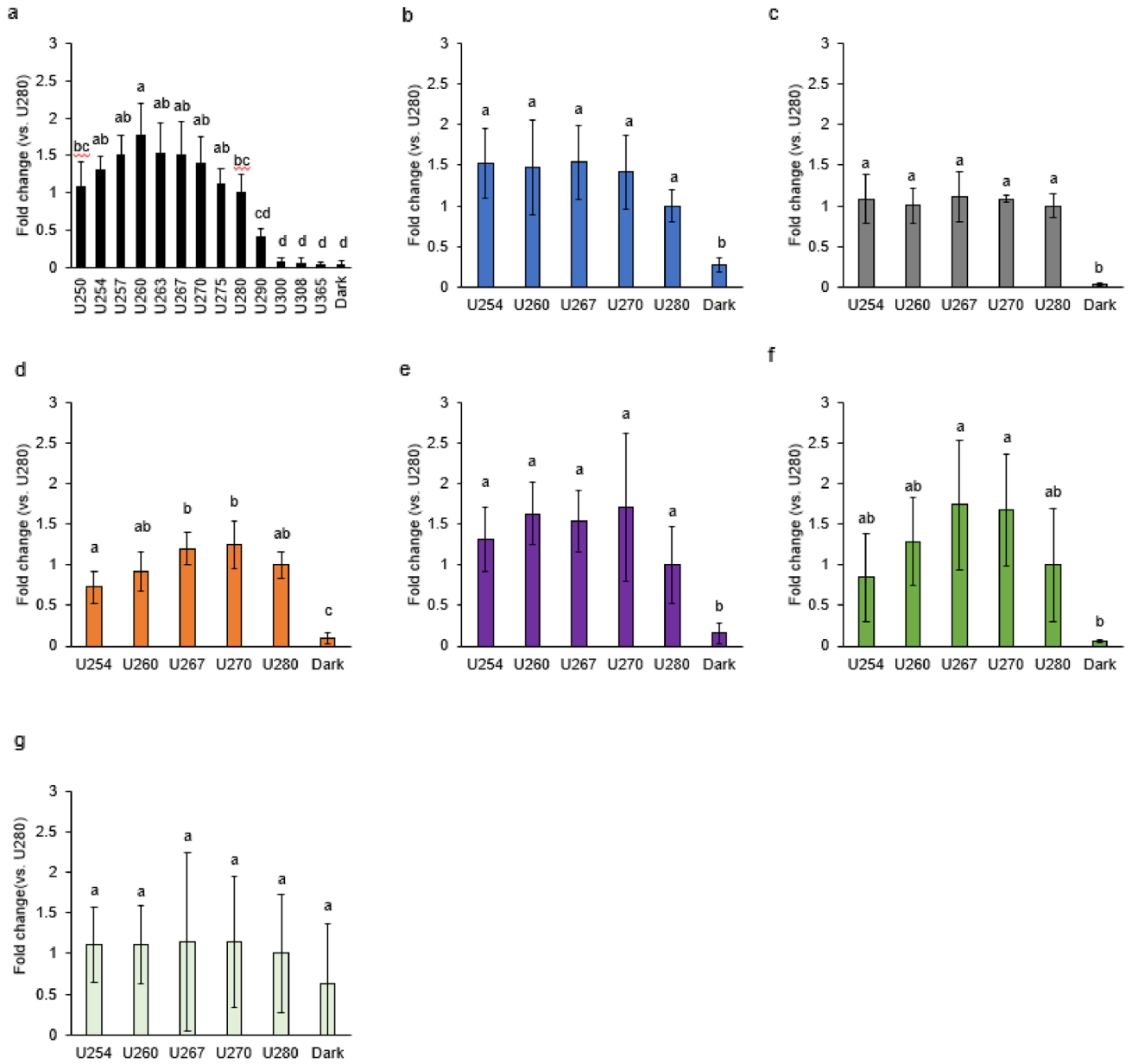

Fig. 3 Relative cyclobutane pyrimidine dimer (CPD) levels in bacteria irradiated with U254, U260, U267, U270, and U280 LEDs. CPD was measured at the fluence resulting by a factor of 1 $\log_{10}$ inactivation for each bacterium after U280 LED irradiation. **a** *E. coli*, **b** *V. parahaemolyticus,* **c** *C. jejuni*, **d** *S. aureus*, **e** *E. faecalis,* **f** *B. subtilis* trophozoite, and **g** *B. subtilis* spore. Results value were showed relative to U280 LED irradiation. P values were determined by one–way ANOVA followed by Tukey's test. Different letters indicate significant differences ($P < 0.05$); n = 4/group

faecalis showed a shift in the log phase at all wavelengths compared with the non-irradiated group. In contrast, *S. aureus* showed a shift in the log phase only under U365 LED irradiation. *B. subtilis* showed a shift in the log phase under the UVB and UVC wavelengths compared with the non-irradiated and U365 LED irradiated groups. *V. parahaemolyticus* showed similar growth curves in all samples, including the control. The slope of the log phase differed significantly compared with the control sample at several wavelengths in each bacterium (Table S4). Similarly, the number of bacteria in the stationary phase was comparable regardless of UV irradiation without *B. subtilis*. These findings suggest that UV irradiation may cause delayed growth onset, leading to a shift in the log phase. Additionally, the wavelengths caused shift in the log phase and this result may vary depending on the bacterial strain.

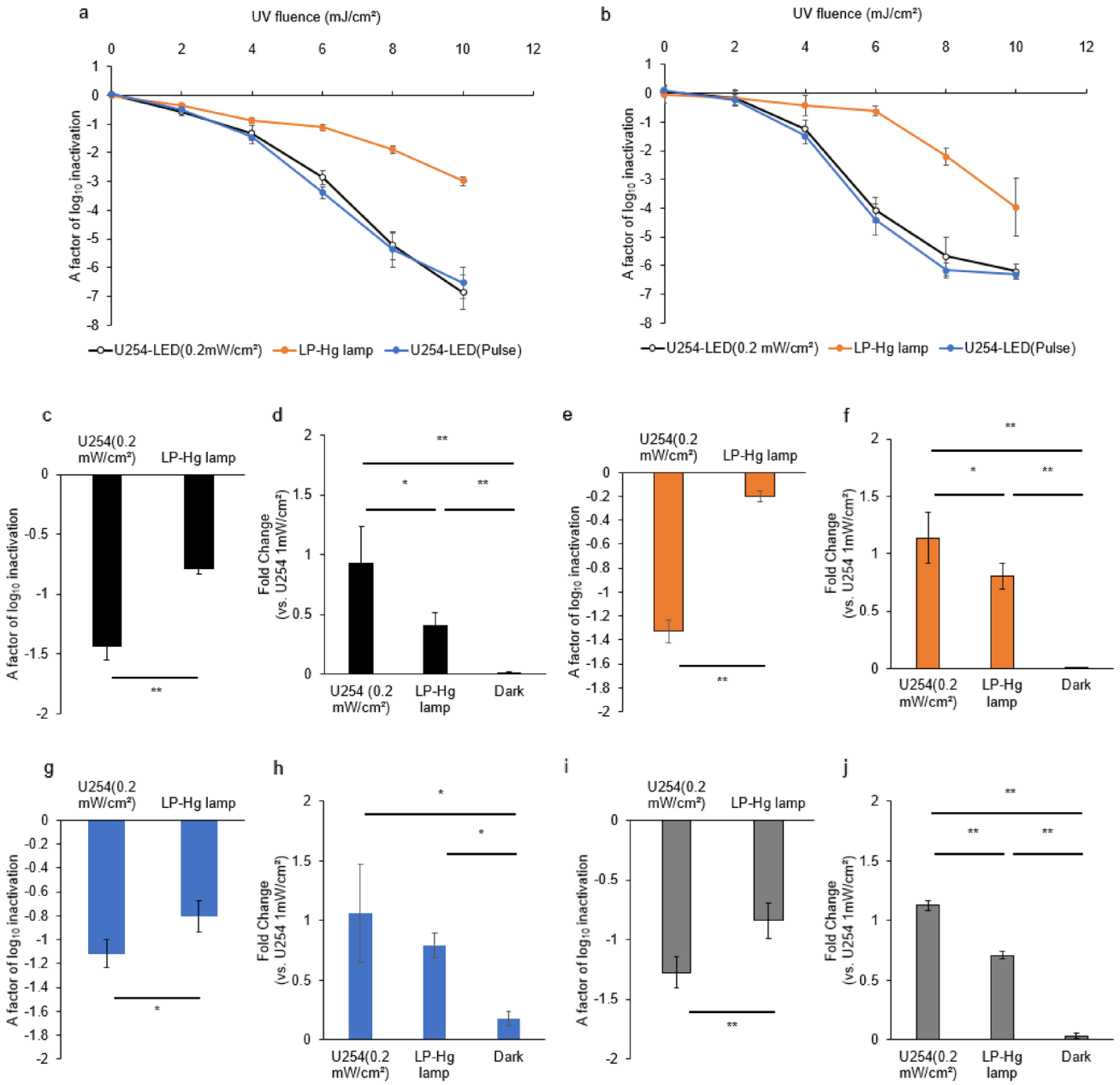

Fig. 4 Differences in bacterial inactivation and CPD production between the UV-LED and LP-Hg lamp under the same UV fluence. **a** Fluence response curves of *E. coli* using continuous irradiation by UV–LED (irradiance of 0.2 mW/cm^2), pulsed irradiation by UV–LED (irradiance of 0.2 mW/cm^2), and the LP-Hg lamp (irradiance of 0.2 mW/cm^2). **b** Fluence response curves of *S. aureus* using continuous irradiation by UV-LED (irradiance of 0.2 mW/cm^2), pulsed irradiation by UV-LED (irradiance of 0.2 mW/cm^2), and the LP–Hg lamp (irradiance of 0.2 mW/cm^2). **c** Bacterial inactivation and **d** CPD production level in *E. coli* at a fluence of 4.5 mJ/cm^2 using the UV–LED and LP–Hg lamp (irradiance of 0.2 mW/cm^2), **e** Bacterial inactivation effect and (f) CPD production level of *S. aureus* at a fluence of 4.2 mJ/cm^2 using UV-LED and LP-Hg lamp (irradiance of 0.2 mW/cm^2), **g** Bacterial inactivation and (h) CPD production in *V. parahaemolyticus* at a fluence of 1.2 mJ/cm^2 using the UV-LED and LP-Hg lamp (irradiance of 0.2 mW/cm^2), **i** Bacterial inactivation and (j) CPD production in *C. jejuni* at a fluence of 2.1 mJ/cm^2 using the UV-LED and LP-Hg lamp (irradiance of 0.2 mW/cm^2). Bar indicate the mean concentration. *P < 0.05, and **P < 0.01, compared with each group (Student's *t* test); n = 4/group

Discussion

Sterilization using UV light is an effective disinfection method for various applications, including disinfection of water, food, and spaces within the human living environment. Until now, LP-Hg lamps have been the most commonly used UV sterilization devices. However, due to restrictions and legislative bans on mercury use, UV–LEDs

Table 2 The results of correlation coefficient and regression analysis for inactivation rate and CPD production

		E. coli	*V. parahaemolyticus*	*C. jejuni*	*S. aureus*	*E. faecalis*	*B. subtilis* trophozoite	*B. subtilis* spore
Correlation coefficient	Correlation coefficient (r)	0.925	0.771	0.943	0.908	0.933	0.943	0.886
	p-value	< 0.001	0.072	0.005	0.012	0.007	0.005	0.019
Regression analysis	R^2	0.909	0.982	0.907	0.825	0.870	0.939	0.837
	Slope (m)	0.635	0.742	0.656	0.402	0.343	0.746	0.130

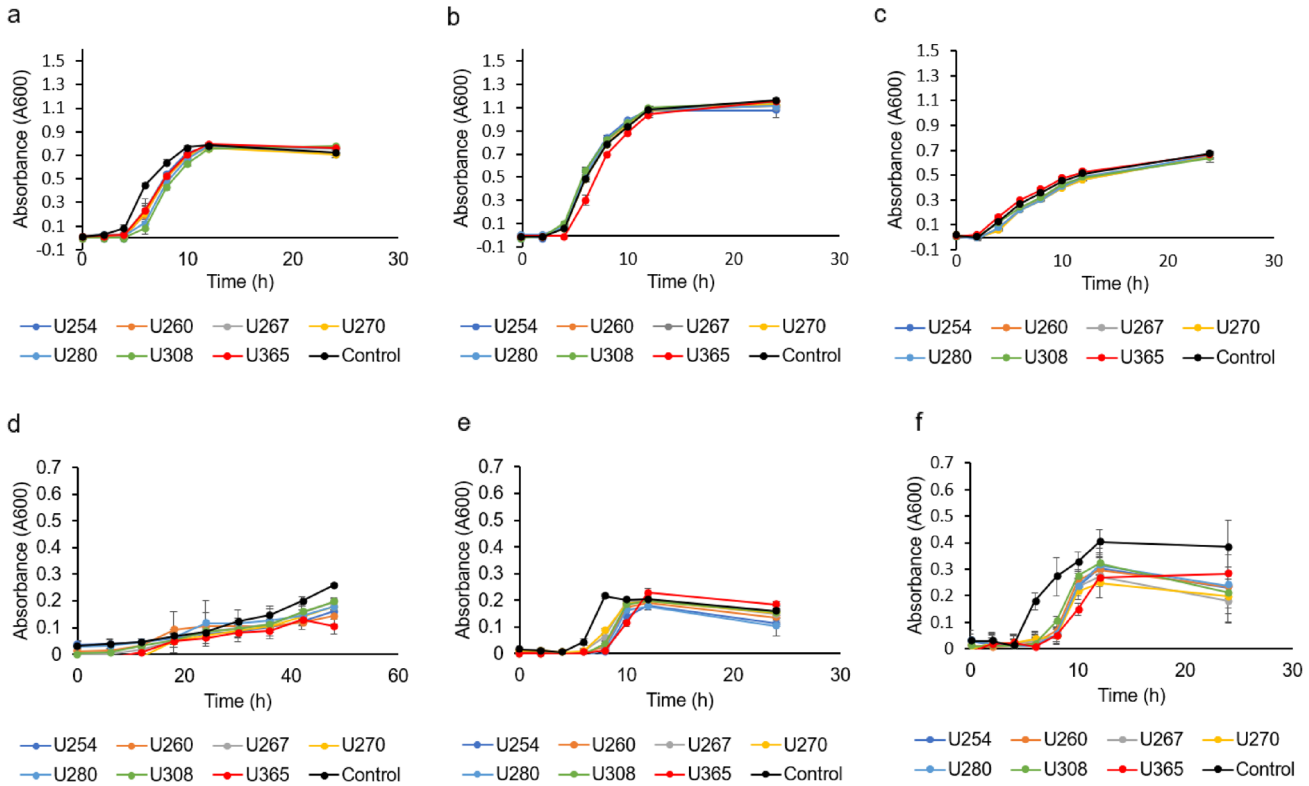

Fig. 5 Bacterial growth curves after UV-LED irradiation. Bacteria were exposed to seven wavelength-ranked LEDs (U254, U260, U267, U270, U280, U308, and U365) at each fluence achieving a factor of 1 $\log_{10}$ inactivation. **a** *E. coli* was irradiated at 2.8 mJ/cm^2 (U254 and U260 LEDs), 2.5 mJ/cm^2 (U267 and U270 LEDs), 4.5 mJ/cm^2 (U280 LED), 480 mJ/cm^2 (U308 LED), and 13.5 J/cm^2 (U365 LED). **b** *S. aureus* was irradiated at 3.5 mJ/cm^2 (U254 LED), 3.0 mJ/cm^2 (U260, U267 and U270 LEDs), 4.2 mJ/cm^2 (U280 LED), 550 mJ/cm^2 (U308 LED), and 16.2 J/cm^2 (U365 LED). **c** *V. parahaemolyticus* was irradiated at 0.8 mJ/cm^2 (U254 and U260 LEDs), 0.7 mJ/cm^2 (U267 and U270 LEDs), 1.2 mJ/cm^2 (U280 LED), 130 mJ/cm^2 (U308 LED), and 3.96 J/cm^2 (U365 LED). **d** *C. jejuni* was irradiated at 1.7 mJ/cm^2 (U254 LED), 1.6 mJ/cm^2 (U260 LED), 1.0 mJ/cm^2 (U267 LED), 1.4 mJ/cm^2 (U270 LED), 2.1 mJ/cm^2 (U280 LED), 260 mJ/cm^2 (U308 LED), and 400 mJ/cm^2 (U365 LED). **e** *E. faecalis* was irradiated at 5.6 mJ/cm^2 (U254 LED), 4.8 mJ/cm^2 (U260 LED), 4.4 mJ/cm^2 (U267 LED), 4.5 mJ/cm^2 (U270 LED), 7.5 mJ/cm^2 (U280 LED), 1000 mJ/cm^2 (U308 LED), and 34.43 J/cm^2 (U365 LED). **f** *B. subtilis* trophozoite was irradiated at 3.7 mJ/cm^2 (U254 LED), 2.8 mJ/cm^2 (U260, U267 and U270 LEDs), 4.5 mJ/cm^2 (U280 LED), 480 mJ/cm^2 (U308 LED), and 40.173 J/cm^2 (U365 LED). Data are presented as the mean ± SD from four independent measurements

are gaining attention for their vast breadth of wavelengths, compact size, versatile design, long lifespan, tunable output (regulated by driving current), and environmental advantages, such as the lack of hazardous waste like mercury. UV–LEDs can be designed to precisely adjust peak wavelengths in increments of a few nanometers. However, bacterial inactivation at wavelengths other than characteristic ones such as 254 and 280 nm has not received much attention. Furthermore, the number of bacteria has been evaluated in terms of UV–LED induced inactivation remains limited (Martín et al. 2023). Therefore, we evaluated the UV sensitivity of ten bacterial strains across a range of UV wavelengths using a newly developed UV–LED device.

First, we measured the dose responses of the 10 bacteria using the U280 LED, which has a peak wavelength of 281.3 nm. All bacteria exhibited dose-dependent inactivation under U280 LED irradiation; however, the inactivation effects at the same UV fluence varied depending on the bacterial strain. A previous study indicated that the integrated UV fluences achieving 2 $\log_{10}$ inactivation of *E. coli, P. aeruginosa, S. aureus,* and *B. subtilis* at a UV wavelength of 285 nm were 9.2, 5.5, 7.1 and 10.8 mJ/cm^2 (Sun et al. 2023), respectively. In comparison, our results showed that all strains required a lower UV fluence to achieve 2 $\log_{10}$ inactivation (Table 2). It is thought that these differences are attributed to the different bacterial strains and equipment conditions between the two studies. In fact, it has been reported that the inactivation effect varies among different strains of the same bacterial species (Masjoudi et al. 2021). Evaluation of bacterial inactivation under the same conditions using this system should clarify the differences in photosensitivity among strains in the future. Furthermore, based on the response curves obtained from the measured data, we evaluated the K_1 and K_2 constants for each bacterium. As a results, K_1 was higher for all Gram-negative than Gram-positive bacteria. Previous studies have suggested that Gram-positive bacteria are less sensitive to UV sterilization compared with Gram–negative bacteria, primarily due to the thickness of the peptidoglycan layer and the absence of an outer membrane (Jaiaue et al. 2022). The peptidoglycan layer of Gram–negative bacteria is a very thin monolayer (8–15 nm), whereas that of Gram-positive bacteria is multilayered and relatively thick (30–80 nm) (Sun et al. 2023). According to those studies, the smaller slope in K_1 that we observed in Gram–positive bacteria under UV irradiation suggests that the thick peptidoglycan layer and absence of an outer membrane influence the initial sensitivity of Gram–positive bacteria to UV irradiance using our UV device. In our study, *E. coli* exhibited weak initial UV sensitivity similar to that of the Gram-positive *S. aureus* and *B. subtilis* trophozoite. Another factor influencing UV sensitivity is the DNA repair mechanism. While DNA damage caused by UV irradiation is repaired primarily by the action of DNA photolyases (Oguma et al. 2001), the effects of DNA photolyases were likely minimal in our study because both irradiation and incubation were conducted under dark conditions. A previous study reported that prokaryotes utilize translesion synthesis (TLS), mainly employing Y-family DNA polymerases, which are lesion-tolerance mechanisms that enable the replication machinery to bypass damaged DNA sites (Fuchs et al. 2013). It has been reported that *E. coli* possesses the *umuC* family DNA polymerase V (*pol V*) as a TLS–type polymerase (Fujii et al. 2004). Pol V is a major polymerase that catalyzes the efficient bypass of UV–induced DNA lesions in the presence of RecA (Duigou et al. 2005; Tang et al. 2000; Pham et al. 2002). Additionally, *B. subtilis* also undergoes TLS using Y-family polymerases (Duigou et al. 2005) and encodes *uvrX*, a member of the Gram-positive *umuC* family, which is phylogenetically close to *pol V* (Ohmori et al. 2001). In contrast, it has been reported that *P. aeruginosa* and *V. cholerae*, which are closely related to *V. parahaemolyticus*, possess *dinP*, a member of the *dinB* family of Y–polymerases; *dinP* mediates untargeted mutagenesis and is required for adaptive mutagenesis (Duigou et al. 2005; Ohmori et al. 2001). These findings suggest that *E. coli*, unlike other Gram–negative bacteria, exhibit weakened inactivation under low UV fluence due to the ability of this strain to perform TLS via TLS-type polymerases, to repair UV-induced DNA damage.

Using UVC LEDs with wavelength increments of a few nanometers to evaluate differences in inactivation effects across the different wavelengths, we found that all bacterial strain exhibited a peak inactivation effect around 263–270 nm (Fig. 2). Since it was reported in some bacteria (Sun et al. 2023; Mamane et al. 2005; Rattanakul et al. 2018), the peak inactivation effect was around 265 nm at the same UV fluence, our results emphasized to these results in more detail. A previous study indicated that bacterial inhibition at 265 or 285 nm was mainly due to DNA damage, specifically the formation of CPDs and 6,4–PPs (Tang et al. 2000). Under natural conditions, CPDs constitute the majority (~75%) of this DNA damage, while 6,4–PPs make up the remaining 25% (Wang et al. 2022). Therefore, measurement of the CPD and 6,4–PP levels in bacterial DNA irradiated at each wavelength indicated that all bacteria, except for the *B. subtilis*, spore showed changes in CPD production corresponding to the changes in inactivation. Our results suggest a correlation between bacterial inactivation and DNA damage, in the form of CPD and 6,4–PP production, in the UVC wavelength range (Figs. 2, 3; Table 3). CPDs result from the binding of thymine to another pyrimidine base within DNA. A previous study indicated that absorption spectrum of thymine peaks at 265 nm (Gustavsson et al. 2006). Therefore, the maximum inactivation observed at 263–270 nm within the UVC region may be attributed to thymine's UV absorption, which indicates CPD production. We simulated the contribution of each wavelength to bacterial inactivation using the deconvolution method based on the measured inactivation of *E. coli*. As a result, a peak in inactivation was calculated around 263–267 nm, which corresponds to the measured inactivation and CPD production results. In addition, subpeaks were observed around 260 and 280 nm (Fig. S6), which correspond to the absorption maximum of RNA/DNA and proteins (especially tyrosine and tryptophan), respectively (Gustavsson et al. 2006; Pivetta et al. 2024; Lavrinenko et al. 2020). Based on these findings, the UV wavelengths showed a greater inactivation effect around 263–267 nm, likely due to CPD production

caused by thymine absorption. On the other hand, higher photosensitivity around 260– and 280– nm, compared with other wavelengths, may be induced by the uracil contest, as well as the tyrosine and tryptophan contents, in bacterial cells. Particularly, differences in sensitivity to wavelengths around 260- and 280-nm due to variations in nucleotide and amino acid compositions may contribute to the differences in UV sensitivity among bacterial strain.

Since there was no significant difference in CPD production between irradiated and non–irradiated *B. subtilis* spore, factors other than CPD production may influence the UV–induced bacterial inactivation to *B. subtilis* spore. *B. subtilis* forms spore under nutrient restricted conditions. These spores exhibit high resistance to heat, chemical, and physical treatments due to their thick proteinaceous coats, peptidoglycan cortex, low water content, high level of dipicolinic acid, and divalent cations in the spore core (Cho et al. 2020). In addition to conventional heat sterilization, non-thermal inactivation processes and chemical inactivation are gaining attention for spore sterilization. Using these inactivation methods, UV irradiation can cause various effects, including abnormal ion flow, increased cell membrane permeability, and cell membrane depolarization (Cho et al. 2012; Gayán et al. 2013; Sun et al. 2016). A previous study indicated that excessive UVC irradiation (25–100 mJ/cm^2) causes DNA damage, and irradiation above 1 mJ/cm^2 led to the denaturation of spore proteins involved in germination (Kuwana et al. 2023). According to those studies, our UV irradiation systems may induce damage of spore DNA related to germination leading to bacterial inactivation via the inhibition of spore germination.

Our data indicated that U254-LED showed greater inhibition of each bacterium compared with the LP-Hg lamp (Fig. 4). In general, the differences between LP-Hg lamps, which have a peak wavelength of 253.4 nm, and UV-LEDs include the emission method and the spectral width of the irradiation wavelengths. These differences likely contributed to the significant variations in bacterial inactivation observed under the same UV fluence in our study. To determine whether the difference in emission method (continuous vs. alternating modes for UV-LEDs vs. LP-Hg lamps) affects the bacterial inactivation ability of each device, we examined the irradiation results for *E. coli*. The UV-LED, when adjusted to the same emission method as that of the LP-Hg lamp, showed no difference in inactivation compared with continuous emission from the UV–LED, indicating that the emission method does not influence bacterial inactivation (Fig. 4a, S4a). The LP-Hg lamp emits monochromatic UV radiation centered around 254 nm, while the U254–LED has a spectral width of approximately 10 nm at half maximum (Fig. S4b). We found that irradiation using the UV–LEDs, each with peak wavelengths differing by only a few nanometers, resulted in differences in inactivation across the wavelengths for all the tested bacteria. These differences were primarily attributed to the amount of DNA damage, such as CPD production (Fig. 2, 3). Additionally, when comparing bacterial inactivation and CPD production between the UV–LEDs and LP-Hg lamp, CPD production was correlated with the bacterial inactivation ability (Fig. 4c-j). These results suggest that the proportion of light at each wavelength contained in the emitted radiation may directly influence the inactivation ability via variations in DNA damage.

Finally, in addition to the evaluation of CPD production, we investigated the change in bacterial growth, 8-OHdG production, and the amount of protein produced immediately after UV irradiation using several wavelengths. The bacterial growth results showed that the time to reach the log phase for *E. coli, C. jejuni,* and *E. faecalis* were delayed at all wavelengths, whereas shifts in the log phase of *S. aureus* and *B. subtilis* were observed especially under U365 LED irradiation. These findings indicate that the wavelengths affecting growth potential differ among bacterial strains (Fig. 5). Previous reports have shown that when damaged *E. coli* is cultured, the period before growth resumes, including the lag phase, is extended to allow repair of the damage (Tsuchido et al. 2023). Additionally, UV irradiation of *E. coli* induces an SOS response, in which the SulA protein inhibits cell division (Burby et al. 2020). Based on these findings, our results suggest that extension of the period before growth resumes, due to induction of the SOS response triggered by UV-induced DNA damage, may have caused the shift in log phase. In contrast, *S. aureus* and *B. subtilis* exhibited a shift in the log phase only after U365 LED irradiation (Fig. 5b). Similar to *E. coli*, *S. aureus* possesses a nucleotide excision repair pathway that repairs DNA damage by the SOS response. The SOS response in *S. aureus* is triggered by the YolD protein, which differs from the protein responsible for SOS activation in *E. coli* (Ha et al. 2021). Since *B. subtilis* relies on YolD for its SOS response (Permina et al. 2002), it is possible that U365 LED irradiation caused a shift in log phase in *B. subtilis*, similar to that in *S. aureus*. This difference in the protein responsible for SOS activation may explain the variation in recovery rates following irradiation at each wavelength. On the other hand, we found no change in the bands of bacterial protein irradiated each wavelength by SDS-PAGE and Native-PAGE, suggesting no change in the number of proteins produced immediately after irradiation (Fig. S3). However, because SDS-PAGE and Native-PAGE assess complete inhibition of protein production, as indicated by a lack of bands (Arakawa et al. 2022), the extent of production of the individual proteins may not have been evaluated adequately. Therefore, to compare the effects of different UV wavelengths on individual protein production in more detail in the future, RNA-seq and other gene expression methods are needed. Furthermore, UVB and UVC wavelengths exert bactericidal effects primarily via direct damage to the target DNA, whereas UVA wavelengths have more indirect effects associated with oxidative damage due to increased intracellular production of ROS such as 8-OHdG (Al-Sadek et al. 2024; Song et al. 2019). In this study, the wavelength used for irradiation was

limited for comparison with CPD productions, but it is possible that 8-OHdG production can be confirmed using LEDs with longer wavelengths. 8-OHdG production was also confirmed by the presence of various cellular photosensitizers, such as flavins, melanin, riboflavin, and porphyrins (Jin et al. 2022); the presence or absence of photosensitizers in each bacterial strain may be affected by 8-OHdG production after UVA irradiation. In addition, other studies have shown significantly lower intracellular ATP levels in *E. coli* than in *S. aureus* after 254 nm UV irradiation, and ATP depletion leads to delayed initiation of DNA replication via degradation of DnaA in *E. coli* (Charbon et al. 2021). Those studies suggested that the intracellular ATP level after UV irradiation influences the rate of subsequent growth. Therefore, further experiments using wavelengths not investigated in this paper are expected to clarify the bacterial inactivation mechanism of each wavelength and ultimately enable the selection of more effective LEDs for each target, contributing to the development of more efficient methods of bacterial growth inhibition.

Conclusions

We investigated the UV sensitivity of various bacterial strains present in human environments and the correlation between effective UV wavelengths and bacterial DNA damage. In the UVC range, bacterial inactivation was dependent on the wavelength, and all tested bacteria showed strong inactivation under UV–LED, which has a peak wavelength around 263–270 nm. CPD production also differed among the UV wavelengths, showing a correlation with the bacterial inactivation effect. In comparison with the LP-Hg lamp, differences in both bacterial inactivation and CPD production were observed under the same irradiation conditions, suggesting that these differences may be due to the wavelength components of the devices. However, since our study evaluated only one strain of bacteria per species, it will be necessary in the future to accumulate data on UV-LED inactivation of other strains in addition to other bacteria. Measurement of the UV sensitivity of each bacterium and the wavelength dependence of bacterial inactivation, as well as the different characteristics of UV–LEDs and LP–Hg lamps observed in this study, will be useful for the development of UV irradiation devices and methods aimed to prevent bacterial infections.

Supplementary Information The online version contains supplementary material available at https://doi.org/10.1007/s00203-025-04324-0.

Author contributions Kai Ishida: Conceptualization, Data curation, Formal analysis, Investigation, Methodology, Writing – original draft. Mina Matsubara: Data curation, Investigation, Methodology, Writing – review & editing. Miharu Nagahashi: Investigation, Methodology. Yushi Onoda: Conceptualization, Methodology, Writing – review & editing. Toshihiko Aizawa: Data curation, Formal analysis, Methodology, Resources. Shigeharu Yamauchi: Conceptualization, Funding acquisition, Investigation, Project administration, Resources, Supervision, Writing – review & editing. Yasuo Fujikawa: Investigation, Resources, Validation, Writing – review & editing. Tomotake Tanaka: Conceptualization, Funding acquisition, Project administration, Resources, Supervision. Yasuko Kadomura-Ishikawa: Methodology, Validation, Investigation. Takashi Uebanso: Writing – review & editing. Masatake Akutagawa: Investigation, Methodology, Software. Kazuaki Mawatari: Conceptualization, Supervision, Writing – review & editing. Akira Takahashi: Conceptualization, Funding acquisition, Supervision, Visualization, Writing – review & editing. All authors commented on previous versions of the manuscript. All authors read and approved the final manuscript.

Funding This work was financially supported by JSPS KAKENHI, grant numbers 23K18578, and by a research grant from Nichia corporation.

Data Availability No datasets were generated or analysed during the current study.

Declarations

Conflict of Interest The authors declare no competing interests.

References

Al-Sadek T, Yusuf N (2024) Ultraviolet radiation biological and medical implications. Curr Issues Mol Biol 46(3):1924–1942. https://doi.org/10.3390/cimb46030126

Antunes P, Novais C, Peixe L (2020) Food-to-humans bacterial transmission. Microbiol Spectr. https://doi.org/10.1128/microbiolspec.mtbp-0019-2016

Arakawa T, Nakagawa M, Tomioka Y, Sakuma C, Li C, Sato T, Sato R, Shibata T, Kurosawa Y, Akuta T (2022) Gel-electrophoresis based method for biomolecular interaction. Methods Cell Biol 169:67–95. https://doi.org/10.1016/bs.mcb.2021.12.030

Beck SE, Linden KG (2015) Protocol for the determination of fluence (UV dose) using a low-pressure or low-pressure high-output UV lamp in bench-scale collimated beam ultraviolet experiments. IUVA News 17:11–17

Beck SE, Rodriguez RA, Linden KG, Hargy TM, Larason TC, Wright HB (2014) Wavelength dependent UV inactivation and DNA damage of adenovirus as measured by cell culture infectivity and long range quantitative PCR. Environ Sci Technol 48(1):591–598. https://doi.org/10.1021/es403850b

Beck SE, Wright HB, Hargy TM, Larason TC, Linden KG (2015) Action spectra for validation of pathogen disinfection in medium-pressure ultraviolet (UV) systems. Water Res 70:27–37. https://doi.org/10.1016/j.watres.2014.11.028

Bharti B, Li H, Ren Z, Zhu R, Zhu Z (2022) Recent advances in sterilization and disinfection technology: a review. Chemosphere 308(Pt 3):136404. https://doi.org/10.1016/j.chemosphere.2022.136404

Blatchley ER (1997) Numerical modelling of UV intensity: application to collimated-beam reactors and continuous-flow systems. Water Res 31:2205–2218. https://doi.org/10.1016/S0043-1354(97)82238-5

Bolton JR, Beck S, Linden KG (2015) Protocol for the determination of fluence (UV dose) using a low-pressure or low-pressure high-output UV lamp in benchscale collimated beam ultraviolet experiments. IUVA News 17:11–17

Burby PE, Simmons LA (2020) Regulation of cell division in bacteria by monitoring genome integrity and DNA replication status. J Bacteriol 202(2):e00408-e419. https://doi.org/10.1128/JB.00408-19

Cascante Vega J, Yaari R, Robin T, Wen L, Zucker J, Uhlemann AC, Pei S, Shaman J (2025) Estimating nosocomial transmission of micro-organisms in hospital settings using patient records and culture data. Epidemics 25(50):100817. https://doi.org/10.1016/j.epidem.2025.100817

Charbon G, Frimodt-Møller J, Løbner-Olesen A (2021) Arresting chromosome replication upon energy starvation in *Escherichia coli*. Curr Genet 67(6):877–882. https://doi.org/10.1007/s00294-021-01202-2

Chen RZ, Craik SA, Bolton JR (2009) Comparison of the action spectra and relative DNA absorbance spectra of microorganisms: information important for the determination of germicidal fluence (UV dose) in an ultraviolet disinfection of water. Water Res 43(20):5087–5096. https://doi.org/10.1016/j.watres.2009.08.032

Chen Q, Liu B, Liu G, Shi H, Wang J (2023) Effect of *Bacillus subtilis* and *Lactobacillus plantarum* on solid-state fermentation of soybean meal. J Sci Food Agric 103(12):6070–6079. https://doi.org/10.1002/jsfa.12683

Cho WI, Chung MS (2020) *Bacillus* spores: a review of their properties and inactivation processing technologies. Food Sci Biotechnol 29(11):1447–1461. https://doi.org/10.1007/s10068-020-00809-4

Cho W-I, Cheigh C-I, Chung M-S, Park K-H, Chang P-S, Chung M-S (2012) The combined effect of UV irradiation and ethanol extract from *Torilis japonica* Fruit on inactivation of bacillus subtilis spores. J Food Saf 32(4):474–480. https://doi.org/10.1111/jfs.12010

Dadashi M, Sharifian P, Bostanshirin N, Hajikhani B, Bostanghadiri N, Khosravi-Dehaghi N, van Belkum A, Darban-Sarokhalil D (2021) The global prevalence of daptomycin, tigecycline, and linezolid-resistant *Enterococcus faecalis* and *Enterococcus faecium* strains from human clinical samples: a systematic review and meta-analysis. Front Med (Lausanne) 10(8):720647. https://doi.org/10.3389/fmed.2021.720647

Delahoy MJ, Shah HJ, Weller DL, Ray LC, Smith K, McGuire S, Trevejo RT, Scallan Walter E, Wymore K, Rissman T, McMillian M, Lathrop S, LaClair B, Boyle MM, Harris S, Zablotsky-Kufel J, Houck K, Devine CJ, Lau CE, Tauxe RV, Bruce BB, Griffin PM, Payne DC (2023) Preliminary incidence and trends of infections caused by pathogens transmitted commonly through food—foodborne diseases active surveillance network, 10 US Sites, 2022. MMWR Morb Mortal Wkly Rep 72(26):701–706. https://doi.org/10.15585/mmwr.mm7226a1.

Duigou S, Ehrlich SD, Noirot P, Noirot-Gros MF (2005) DNA polymerase I acts in translesion synthesis mediated by the Y-polymerases in Bacillus subtilis. Mol Microbiol 57(3):678–690. https://doi.org/10.1111/j.1365-2958.2005.04725.x

Erkan Alkan P, Karabiyik T (2025) Nanobubble ozone stored in hyaluronic acid-decorated liposome solutions: inactivating antibiotic-resistant bacteria and genotoxicity, sub-acute and sub-chronic toxicity tests. Infect Drug Resist 16(18):313–328. https://doi.org/10.2147/IDR.S478643

Fuchs RP, Fujii S (2013) Translesion DNA synthesis and mutagenesis in prokaryotes. Cold Spring Harb Perspect Biol 5(12):a012682. https://doi.org/10.1101/cshperspect.a012682

Fujii S, Gasser V, Fuchs RP (2004) The biochemical requirements of DNA polymerase V-mediated translesion synthesis revisited. J Mol Biol 341(2):405–417. https://doi.org/10.1016/j.jmb.2004.06.017

Fukushima S, Shimohata T, Inoue Y, Kido J, Uebanso T, Mawatari K, Takahashi A (2022) Recruitment of LC3 by *Campylobacter jejuni* to bacterial invasion site on host cells *via* the Rac1-mediated signaling pathway. Front Cell Infect Microbiol 3(12):829682. https://doi.org/10.3389/fcimb.2022.829682

Gayán E, Álvarez I, Condón S (2013) Inactivation of bacterial spores by UV-C light. Innov Food Sci Emerg Technol 19:140–145. https://doi.org/10.1016/j.ifset.2013.04.007

Geeraerd AH, Valdramidis VP, Van Impe JF (2005) GInaFiT, a freeware tool to assess non-log-linear microbial survivor curves. Int J Food Microbiol 102(1):95–105. https://doi.org/10.1016/j.ijfoodmicro.2004.11.038

Gustavsson T, Bányász A, Lazzarotto E, Markovitsi D, Scalmani G, Frisch MJ, Barone V, Improta R (2006) Singlet excited-state behavior of uracil and thymine in aqueous solution: a combined experimental and computational study of 11 uracil derivatives. J Am Chem Soc 128(2):607–619. https://doi.org/10.1021/ja056181s

Ha KP, Edwards AM (2021) DNA repair in *Staphylococcus aureus*. Microbiol Mol Biol Rev 85(4):e0009121. https://doi.org/10.1128/MMBR.00091-21

Hritonenko V, Metruccio M, Evans D, Fleiszig S (2018) Epithelial cell lysates induce ExoS expression and secretion by Pseudomonas aeruginosa. FEMS Microbiol Lett. 365(8):fny53. https://doi.org/10.1093/femsle/fny053

Iliadi V, Staykova J, Iliadis S, Konstantinidou I, Sivykh P, Romanidou G, Vardikov DF, Cassimos D, Konstantinidis TG (2022) *Legionella pneumophila*: the journey from the environment to the blood. J Clin Med 11(20):6126. https://doi.org/10.3390/jcm11206126

Ishida K, Shimohata T, Kanda Y, Nguyen AQ, Masuda R, Yamazaki K, Uebanso T, Mawatari K, Kashimoto T, Takahashi A (2023) Characteristic metabolic changes in skeletal muscle due to vibrio vulnificus infection in a wound infection model. Systems. 8(2):e0068222. https://doi.org/10.1128/msystems.00682-22

Ishida K, Onoda Y, Kadomura-Ishikawa Y, Nagahashi M, Yamashita M, Fukushima S, Aizawa T, Yamauchi S, Fujikawa Y, Tanaka T, Uebanso T, Akutagawa M, Mawatari K, Takahashi A (2024) Development of a standard evaluation method for microbial UV sensitivity using light-emitting diodes. Heliyon 10(6):e27456. https://doi.org/10.1016/j.heliyon.2024.e27456

Jaiaue P, Piluk J, Sawattrakool K, Thammakes J, Malasuk C, Thitiprasert S, Thongchul N, Siwamogsatham S (2022) Mathematical modeling for evaluating inherent parameters affecting UVC decontamination of indicator bacteria. Appl Environ Microbiol 88(7):e0214821. https://doi.org/10.1128/aem.02148-21

Jiang Y, Rabbi M, Kim M, Ke C, Lee W, Clark RL, Mieczkowski PA, Marszalek PE (2009) UVA generates pyrimidine dimers in DNA directly. Biophys J 96(3):1151–1158. https://doi.org/10.1016/j.bpj.2008.10.030

Jin SG, Padron F, Pfeifer GP (2022) UVA radiation, DNA damage, and melanoma. ACS Omega 7(37):32936–32948. https://doi.org/10.1021/acsomega.2c04424

Kebbi Y, Muhammad AI, Santana AS, Do Prado-Silva L, Liu D, Ding T (2020) Recent advances on the application of UV-LED technology for microbial inactivation: Progress and mechanism. Compr Rev Food Sci Food Saf 19(6):3501–3527. https://doi.org/10.1111/1541-4337.12645

Kheyrandish A, Mohseni M, Taghipour F (2018) Protocol for determining ultraviolet light emitting diode (UV-LED) fluence for microbial inactivation studies. Environ Sci Technol 52(13):7390–7398. https://doi.org/10.1021/acs.est.7b05797

Kraft S, Obst U, Schwartz T (2011) Immunological detection of UV induced cyclobutane pyrimidine dimers and (6–4) photoproducts in DNA from reference bacteria and natural aquatic populations. J Microbiol Methods 84(3):435–441. https://doi.org/10.1016/j.mimet.2011.01.004

Kuluncsics Z, Perdiz D, Brulay E, Muel B, Sage E (1999) Wavelength dependence of ultraviolet-induced DNA damage distribution: involvement of direct or indirect mechanisms and possible artefacts. J Photochem Photobiol B 49(1):71–80. https://doi.org/10.1016/S1011-1344(99)00034-2

Kundra S, Lam LN, Kajfasz JK, Casella LG, Andersen MJ, Abranches J, Flores-Mireles AL, Lemos JA (2021) c-di-AMP Is essential for the virulence of *Enterococcus faecalis*. Infect Immun 89(11):e0036521. https://doi.org/10.1128/IAI.00365-21

Kuwana R, Yamazawa R, Asada R, Ito K, Furuta M, Takamatsu H (2023) Excessive ultraviolet C irradiation causes spore protein denaturation and prohibits the initiation of spore germination in Bacillus subtilis. J Microorg Control 28(1):15–25. https://doi.org/10.4265/jmc.28.1_15

Kysela DT, Randich AM, Caccamo PD, Brun YV (2016) Diversity takes shape: understanding the mechanistic and adaptive basis of bacterial morphology. PLoS Biol 14(10):e1002565. https://doi.org/10.1371/journal.pbio.1002565

Lavrinenko IA, Holyavka MG, Chernov VE, Artyukhov VG (2020) Second derivative analysis of synthesized spectra for resolution and identification of overlapped absorption bands of amino acid residues in proteins: bromelain and ficin spectra in the 240–320 nm range. Spectrochim Acta A Mol Biomol Spectrosc 227:117722. https://doi.org/10.1016/j.saa.2019.117722. (**Epub 2019 Oct 31**)

Lawrence KP, Delinasios GJ, Premi S, Young AR, Cooke MS (2022) Perspectives on cyclobutane pyrimidine dimers-rise of the dark dimers. Photochem Photobiol 98(3):609–616. https://doi.org/10.1111/php.13551

Li X, Cai M, Wang L, Niu F, Yang D, Zhang G (2019) Evaluation survey of microbial disinfection methods in UV-LED water treatment systems. Sci Total Environ 659:1415–1427. https://doi.org/10.1016/j.scitotenv.2018.12.344

Liu C, Shen Y, Yang M, Chi K, Guo N (2022) Hazard of staphylococcal enterotoxins in food and promising strategies for natural products against virulence. J Agric Food Chem 70(8):2450–2465. https://doi.org/10.1021/acs.jafc.1c06773

Mafart P, Couvert O, Gaillard S, Leguerinel I (2002) On calculating sterility in thermal preservation methods: application of the Weibull frequency distribution model. Int J Food Microbiol 72(1–2):107–113. https://doi.org/10.1016/s0168-1605(01)00624-9

Mamane-Gravetz H, Linden KG, Cabaj A, Sommer R (2005) Spectral sensitivity of Bacillus subtilis spores and MS2 coliphage for validation testing of ultraviolet reactors for water disinfection. Environ Sci Technol 39(20):7845–7852. https://doi.org/10.1021/es048446t

Martín-Sómer M, Pablos C, Adán C, van Grieken R, Marugán J (2023) A review on LED technology in water photodisinfection. Sci Total Environ 885:163963. https://doi.org/10.1016/j.scitotenv.2023.163963

Masjoudi M, Mohseni M, Bolton JR (2021) Sensitivity of bacteria, protozoa, viruses, and other microorganisms to ultraviolet radiation. J Res Natl Inst Stand Technol 126:126021. https://doi.org/10.6028/jres.126.021

Mežnarić S, Brčić Karačonji I, Crnković G, Lesar A, Pavlešić T, Vučković D, Gobin I (2022) Combined inhibitory effect of Fir (*Abies alba* Mill.) honeydew honey and probiotic bacteria *Lactiplantibacillus plantarum* on the growth of *Salmonella enterica* Serotype Typhimurium. Antibiot (Basel). 11(2):145

Mori M, Hamamoto A, Takahashi A, Nakano M, Wakikawa N, Tachibana S, Ikehara T, Nakaya Y, Akutagawa M, Kinouchi Y (2007) Development of a new water sterilization device with a 365 nm UV-LED. Med Biol Eng Comput 45(12):1237–1241. https://doi.org/10.1007/s11517-007-0263-1

Murat S, Rüya TK (2023) Modelling of *E. coli* inactivation from solutions using GInaFiT via hybrid electrode connected electro-disinfection process. Bilge Int J Sci Technol Res 7(2):142–155

Nakano M, Yamasaki E, Ichinose A, Shimohata T, Takahashi A, Akada JK, Nakamura K, Moss J, Hirayama T, Kurazono H (2012) Salmonella enterotoxin (Stn) regulates membrane composition and integrity. Dis Model Mech 5(4):515–521. https://doi.org/10.1242/dmm.009324

Nascimento É, da Silva SH, Marques Edos R, Roberts DW, Braga GU (2010) Quantification of cyclobutane pyrimidine dimers induced by UVB radiation in conidia of the fungi *Aspergillus fumigatus*, *Aspergillus nidulans*, *Metarhizium acridum* and *Metarhizium robertsii*. Photochem Photobiol 86(6):1259–1266. https://doi.org/10.1111/j.1751-1097.2010.00793.x

Ning P, Han Y, Liu Y, Liu S, Sun Z, Wang X, Wang B, Gao F, Wang Y, Wang Y, Gao X, Chen G, Li X (2023) Study on disinfection effect of a 222-nm UVC excimer lamp on object surface. AMB Express 13(1):102. https://doi.org/10.1186/s13568-023-01611-1

Nyangaresi PO, Rathnayake T, Beck SE (2023) Evaluation of disinfection efficacy of single UV-C, and UV-A followed by UV-C LED irradiation on *Escherichia coli*, *B. spizizenii* and MS2 bacteriophage, in water. Sci Total Environ. 859(Pt 1):160256. https://doi.org/10.1016/j.scitotenv.2022.160256

Oguma K, Katayama H, Mitani H, Morita S, Hirata T, Ohgaki S (2001) Determination of pyrimidine dimers in Escherichia coli and Cryptosporidium parvum during UV light inactivation, photoreactivation, and dark repair. Appl Environ Microbiol 67(10):4630–4637. https://doi.org/10.1128/AEM.67.10.4630-4637.2001

Ohmori H, Friedberg EC, Fuchs RP, Goodman MF, Hanaoka F, Hinkle D, Kunkel TA, Lawrence CW, Livneh Z, Nohmi T, Prakash L, Prakash S, Todo T, Walker GC, Wang Z, Woodgate R (2001) The Y-family of DNA polymerases. Mol Cell 8(1):7–8. https://doi.org/10.1016/s1097-2765(01)00278-7

Oliveira BR, Marques AP, Ressurreição M, Moreira CJS, Pereira SC, Crespo BMT, Pereira VJ (2021) Inactivation of *Aspergillus* species in real water matrices using medium pressure mercury lamps. J Photochem Photobiol B. 221:112242. https://doi.org/10.1016/j.jphotobiol.2021.112242

Onoda Y, Nagahashi M, Yamashita M, Fukushima S, Aizawa T, Yamauchi S, Fujikawa Y, Tanaka T, Kadomura-Ishikawa Y, Ishida K, Uebanso T, Mawatari K, Blatchley ER 3rd, Takahashi A (2024) Accumulated melanin in molds provides wavelength-dependent UV tolerance. Photochem Photobiol Sci 9:1791–1806. https://doi.org/10.1007/s43630-024-00632-4

Park SK, Jo DM, Kang MG, Khan F, Hong SD, Kim CY, Kim YM, Ryu UC (2021) Bactericidal effect of ultraviolet C light-emitting diodes: Optimization of efficacy toward foodborne pathogens in water. J Photochem Photobiol B 222:112277. https://doi.org/10.1016/j.jphotobiol.2021.112277

Pedraza-Reyes M, Abundiz-Yañez K, Rangel-Mendoza A, Martínez LE, Barajas-Ornelas RC, Cuéllar-Cruz M, Leyva-Sánchez HC, Ayala-García VM, Valenzuela-García LI, Robleto EA (2024) Bacillus subtilis stress-associated mutagenesis and developmental

DNA repair. Microbiol Mol Biol Rev 88(2):e0015823. https://doi.org/10.1128/mmbr.00158-23
Permina EA, Mironov AA, Gelfand MS (2002) Damage-repair error-prone polymerases of eubacteria: association with mobile genome elements. Gene 293(1–2):133–140. https://doi.org/10.1016/s0378-1119(02)00701-1
Pham P, Seitz EM, Saveliev S, Shen X, Woodgate R, Cox MM, Goodman MF (2002) Two distinct modes of RecA action are required for DNA polymerase V-catalyzed translesion synthesis. Proc Natl Acad Sci USA 99(17):11061–11066. https://doi.org/10.1073/pnas.172197099
Pham TM, Kretzschmar M, Bertrand X, Bootsma M; COMBACTE-MAGNET Consortium (2019) Tracking Pseudomonas aeruginosa transmissions due to environmental contamination after discharge in ICUs using mathematical models. PLoS Comput Biol 15(8):e1006697. https://doi.org/10.1371/journal.pcbi.1006697
Pivetta TP, Ribeiro PA, Raposo M (2024) The effect of UV–Vis radiation on DNA systems containing the photosensitizers methylene blue and acridine orange. Biophysica. https://doi.org/10.3390/biophysica4010002
Press WH, Teukolsky SA, Vetterling WT, Flannery BP (1992) Numerical recipes in C : the art of scientific computing. Cambridge University Press, Cambridge
Rappaport HB, Oliverio AM (2023) Extreme environments offer an unprecedented opportunity to understand microbial eukaryotic ecology, evolution, and genome biology. Nat Commun 14(1):4959. https://doi.org/10.1038/s41467-023-40657-4
Rastogi RP, Richa KA, Tyagi MB, Sinha RP (2010) Molecular mechanisms of ultraviolet radiation-induced DNA damage and repair. J Nucl Acids 2010:592980. https://doi.org/10.4061/2010/592980
Rattanakul S, Oguma K (2018) Inactivation kinetics and efficiencies of UV-LEDs against *Pseudomonas aeruginosa*, Legionella pneumophila, and surrogate microorganisms. Water Res 130:31–37. https://doi.org/10.1016/j.watres.2017.11.047
Rodríguez RA, Navar C, Sangsanont J, Linden KG (2022) UV inactivation of sewage isolated human adenovirus. Water Res 30(218):118496. https://doi.org/10.1016/j.watres.2022.118496
Schuit MA, Larason TC, Krause ML, Green BM, Holland BP, Wood SP, Grantham S, Zong Y, Zarobila CJ, Freeburger DL, Miller DM, Bohannon JK, Ratnesar-Shumate SA, Blatchley ER 3rd, Li X, Dabisch PA, Miller CC (2022) SARS-CoV-2 inactivation by ultraviolet radiation and visible light is dependent on wavelength and sample matrix. J Photochem Photobiol B 233:112503. https://doi.org/10.1016/j.jphotobiol.2022.112503
Shen C, Fang S, Bergstrom DE, Blatchley ER 3rd (2005) (E)-5-[2-(methoxycarbonyl)ethenyl]cytidine as a chemical actinometer for germicidal UV radiation. Environ Sci Technol 39(10):3826–3832. https://doi.org/10.1021/es049120n
Sholtes K, Keliher R, Linden KG (2019) Standardization of a UV LED peak wavelength, emission spectrum, and irradiance measurement and comparison protocol. Environ Sci Technol 53(16):9755–9763. https://doi.org/10.1021/acs.est.9b02567
Song K, Mohseni M, Taghipour F (2016) Application of ultraviolet light-emitting diodes (UV-LEDs) for water disinfection: a review. Water Res 94:341–349. https://doi.org/10.1016/j.watres.2016.03.003
Song K, Mohseni M, Taghipour F (2019) Mechanisms investigation on bacterial inactivation through combinations of UV wavelengths. Water Res 163:114875. https://doi.org/10.1016/j.watres.2019.114875
Soni J, Sinha S, Pandey R (2004) Understanding bacterial pathogenicity: a closer look at the journey of harmful microbes. Front Microbiol 15:1370818. https://doi.org/10.3389/fmicb.2024.1370818
Sun P, Tyree C, Huang CH (2016) Inactivation of *Escherichia coli*, bacteriophage MS2, and bacillus spores under UV/H_2O_2 and UV/peroxydisulfate advanced disinfection conditions. Environ Sci Technol 50(8):4448–4458. https://doi.org/10.1021/acs.est.5b06097
Sun W, Jing Z, Zhao Z, Yin R, Santoro D, Mao T, Lu Z (2023) Dose-response behavior of pathogens and surrogate microorganisms across the ultraviolet-c spectrum: inactivation efficiencies, action spectra, and mechanisms. Environ Sci Technol 57(29):10891–10900. https://doi.org/10.1021/acs.est.3c00518
Taghipour F (2018) UV LED technology: the times they are A-Changin'. IUVA News 20(1):14–17
Tang M, Pham P, Shen X, Taylor JS, O'Donnell M, Woodgate R, Goodman MF (2000) Roles of *E. coli* DNA polymerases IV and V in lesion-targeted and untargeted SOS mutagenesis. Nature 404(6781):1014–8. https://doi.org/10.1038/35010020
Thomas J, Dirk P, Volker B, Christian W (2016) Deconvolution of time series in the laboratory. Am J Phys 84(10):752–763. https://doi.org/10.1119/1.4960294
Tsuchido T (2023) Injury modes and physiological characteristics of injured microorganisms with a special reference to heat injury. J Microorg Control 28(4):187–200. https://doi.org/10.4265/jmc.28.4_187
Vaseghi SV (2008) Advanced digital signal processing and noise reduction. Wiley, Hoboken. https://doi.org/10.1002/9780470740156 (**ISBN:9780470740156**)
Vetchapitak T, Misawa N (2019) Current status of *Campylobacter* food poisoning in Japan. Food Saf (Tokyo) 7(3):61–73. https://doi.org/10.14252/foodsafetyfscj.D-19-00001
Vollmer W, Blanot D, de Pedro MA (2008) Peptidoglycan structure and architecture. FEMS Microbiol Rev 32(2):149–167. https://doi.org/10.1111/j.1574-6976.2007.00094.x
Wan Q, Cao R, Wen G, Xu X, Xia Y, Wu G, Li Y, Wang J, Xu H, Lin Y, Huang T (2022) Efficacy of UV-LED based advanced disinfection processes in the inactivation of waterborne fungal spores: kinetics, photoreactivation, mechanism and energy requirements. Sci Total Environ 803:150107. https://doi.org/10.1016/j.scitotenv.2021.150107
Wang Y, Deng X, Zhou M (2022) DNA damage mediated by UV radiation and relative repair mechanisms in mammals. Genome Instab Dis 3:331–337. https://doi.org/10.1007/s42764-022-00090-1
Wei J, Li Y (2016) Airborne spread of infectious agents in the indoor environment. Am J Infect Control 44(9 Suppl):S102–S108. https://doi.org/10.1016/j.ajic.2016.06.003. (**PMID:27590694;PMCID: PMC7115322**)
Wibowo JT, Bayu A, Aryati WD, Fernandes C, Yanuar A, Kijjoa A, Putra MY (2023) Secondary metabolites from marine-derived bacteria with antibiotic and antibiofilm activities against drug-resistant pathogens. Mar Drugs 21(1):50. https://doi.org/10.3390/md21010050
Wiener N (1949) Extrapolation, interpolation, and smoothing of stationary time series. The MIT Press, Cambridge. https://doi.org/10.7551/mitpress/2946.001.0001